
Reinforcing Numerical Reasoning in LLMs for Tabular Prediction via Structural Priors

Pengxiang Cai¹ Zihao Gao¹ Wanchen Lian¹ Jintai Chen¹

Abstract

Tabular prediction traditionally relies on gradient-boosted decision trees and deep learning models, which excel in specific tasks but lack interpretability and transferability. Reasoning large language models (LLMs) promise cross-task adaptability with transparent reasoning traces, yet their potential for tabular data remains unrealized. To bridge this gap, we propose a reasoning framework centered on Permutation Relative Policy Optimization (PRPO), a reinforcement learning method that encodes column-permutation invariance as a structural prior. By estimating advantages across label-preserving permutations, PRPO transforms sparse rewards into dense signals, activating latent numerical reasoning capabilities of LLMs with limited supervision. Extensive experiments show that our method matches fully supervised baselines and dominates in zero-shot settings, performing on par with 32-shot strong baselines. Remarkably, our **8B** model significantly outperforms much larger LLMs, achieving up to a **53.17%** improvement over DeepSeek-R1 (**685B**).

1. introduction

Tabular prediction is a central task in machine learning with wide-ranging applications in healthcare, finance, and recommendation systems. Recent advances, including decision tree-based models (Chen & Guestrin, 2016; Prokhorenkova et al., 2018) and deep learning models (Hollmann et al., 2023; 2025; Chen et al., 2022; 2024; Gorishniy et al., 2021), have delivered strong performance on benchmark datasets. However, most of these approaches remain constrained by limited cross-task generalization, perform poorly in zero-shot and few-shot settings, and offer limited interpretability (Ke et al., 2017; Prokhorenkova et al., 2018), thereby

impeding their deployment in real-world scenarios.

Large language models (LLMs) present a new paradigm for tabular prediction. Beyond producing predictive outcomes, LLMs can produce reasoning chains, thereby enhancing transparency and trust. Their pretraining on large-scale, multi-domain corpora also endows them with strong cross-task generalization (Brown et al., 2020; Wei et al., 2022; Wang et al., 2023), enabling rapid adaptation to new tasks under few-shot and zero-shot conditions. However, this potential has not yet been fully realized for tabular data. We argue that one of the key obstacle lies in the modality gap in reasoning: the reasoning patterns learned from natural language and mathematical corpora do not directly transfer to table-specific reasoning, which requires both semantic and numeric understanding. Therefore, bridging this gap by reinforcing numerical understanding and reasoning capabilities is crucial for fully unlocking the latent reasoning potential of LLMs in tabular prediction.

Recently, reinforcement learning (RL) (Schulman et al., 2017; Ouyang et al., 2022; Bai et al., 2022; Rafailov et al., 2023; Shao et al., 2024; DeepSeek-AI et al., 2025) has become a key approach for enhancing the reasoning ability of LLMs. Models such as DeepSeek-R1 (Shao et al., 2024; DeepSeek-AI et al., 2025) demonstrate that Group Relative Policy Optimization (GRPO) can substantially improve long-chain reasoning by leveraging group-relative advantage estimation. Yet, as widely observed when LLMs are extended beyond text (*e.g.*, visual LLMs) (Yao et al., 2025), tabular LLMs struggle to replicate these significant gains due to the sparse-reward problem, stemming from the lack of process-level guidance and the scarcity of positive rewards during RL rollouts, as evidenced by DeepSeek-R1 (685B) achieving only about 57% accuracy on binary classification tasks. Unable to extract effective guidance from such sparse feedback, tabular LLMs fail to capture intrinsic tabular structures, leading to inefficient exploration and severely limiting their few-shot generalization capabilities.

To address this issue, we propose **Permutation Relative Policy Optimization (PRPO)**, a reinforcement learning method specifically designed for tabular prediction, aimed at enhancing reward signals during the RL process via structural priors, thereby improving the numerical reasoning

¹AI Thrust, Information Hub, The Hong Kong University of Science and Technology(Guangzhou). Correspondence to: Jintai Chen <jintaiCHEN@hkust-gz.edu.cn>.

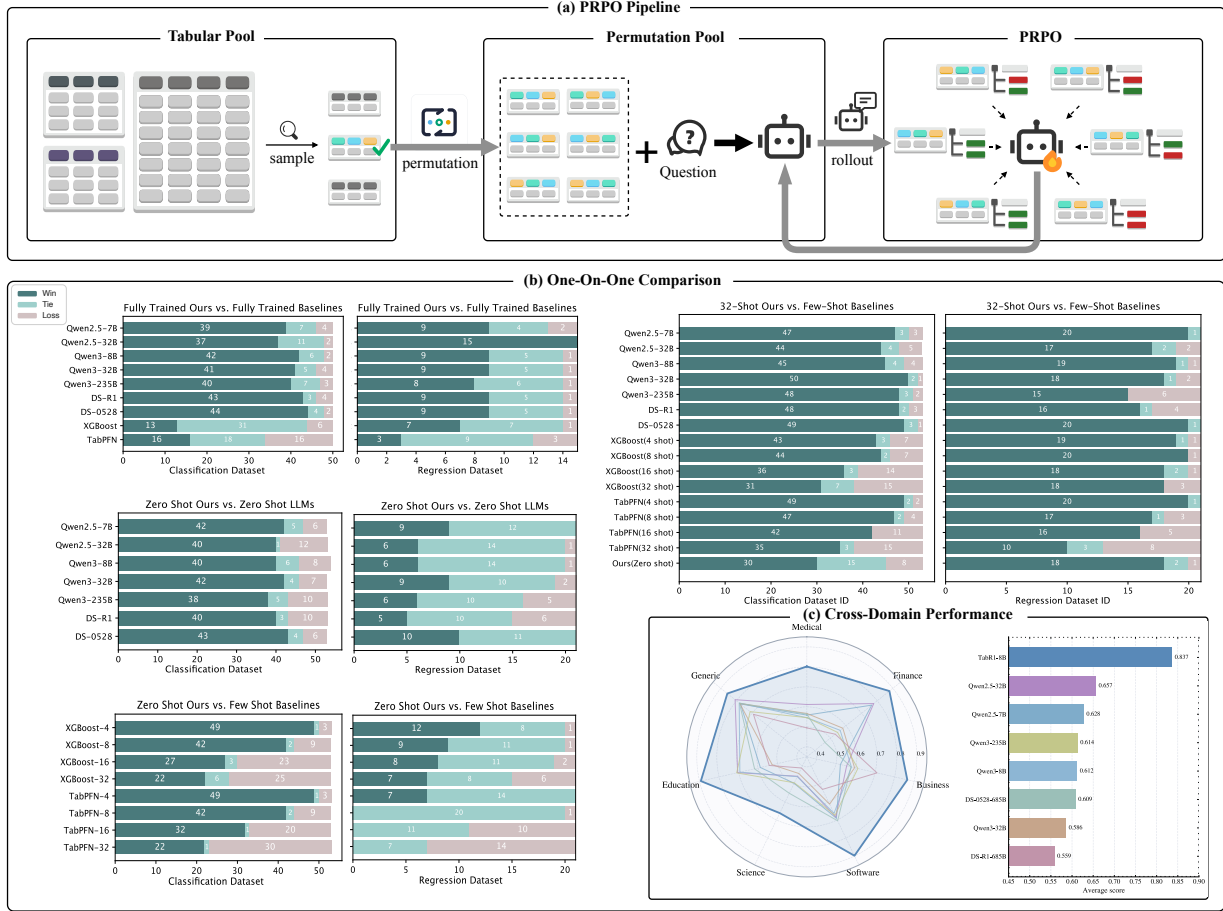


Figure 1. (a) We collect 139 datasets to construct a PRPO-compatible reinforcement learning dataset. Each training sample is permuted into multiple variants, paired with a prediction question, and fed into our model. The rollouts generate both intra-permutation and inter-permutation rewards, providing effective optimization signals for our model. (b) Win–Tie–Loss comparison between our method and other models under fully trained, few-shot, and zero-shot settings. (c) Cross-domain performance of our method and seven LLMs across seven distinct domains.

and understanding capabilities of LLMs. As shown in Figure 1(a), PRPO leverages the structural prior that tabular semantics remain invariant under column permutations. For each sample, it generates multiple column-permuted variants and serializes their feature names and values into reasoning instructions for the LLM. Advantages are then estimated both within and across permutations, providing richer supervisory signals from the same training sample. This mechanism converts sparse outcome-level feedback into denser learning signals while preserving reward fidelity. By operationalizing permutation invariance in this manner, PRPO mitigates inefficient exploration, stabilizes optimization, and markedly improves the generalization ability of LLMs in tabular prediction. Building upon PRPO, we develop the first reasoning LLM for tabular prediction, which not only activates the latent numerical reasoning capacity

of LLMs but also achieves strong zero-shot and few-shot performance with enhanced interpretability. Figure 1(b) and Figure 1(c) present the overall performance comparison between our method and multiple baselines, highlighting the superior capability of our approach. Our contributions are summarized as follows:

(i) We introduce the first reasoning LLM tailored for tabular prediction, which possesses strong numerical reasoning capabilities and integrates tabular semantics with multi-step reasoning to produce precise and interpretable predictions. At the same time, we construct a dataset for reinforcement learning with verifiable rewards to support the training of our model, which also provides an essential data foundation for future tabular reasoning LLMs.

(ii) We propose Permutation Relative Policy Optimiza-

tion (PRPO), a novel reinforcement learning strategy that exploits column-permutation invariance to convert sparse outcome-level rewards into dense learning signals, thereby stabilizing training, improving generalization, and activating the numerical understanding and reasoning capabilities of LLMs with limited supervision.

(iii) We validate that our method achieves strong performance under full supervision and competitive results in few-shot learning, while in the zero-shot setting it substantially outperforms all competitors and even approaches the 32-shot performance of strong baselines such as XGBoost and TabPFN-v2. Moreover, our model surpasses models two orders of magnitude larger while maintaining transparent reasoning traces.

2. Method

We propose the first reasoning LLM tailored for tabular prediction. Previous LLM-based tabular prediction methods have mainly relied on supervised fine-tuning (Hegselmann et al., 2023; Gardner et al., 2024) or prompt engineering (Wei et al., 2022; Wang et al., 2023; Brown et al., 2020). Although these methods bring certain performance improvements, they still fail to fully unlock the reasoning potential of LLMs in tabular prediction. In contrast, we propose Permutation Relative Policy Optimization (PRPO), which effectively activates the numerical reasoning capabilities of LLMs, thereby enhancing performance in tabular prediction. Our method comprises two key stages: (1) **Tabular serialization**. LLMs cannot directly process structured tabular data, as they are primarily trained on unstructured text. To address this, we serialize tabular data into a natural language format suitable for LLM input. Based on this serialization, we constructed a reinforcement learning dataset, enabling reinforcement learning with verifiable rewards. (2) **PRPO fine-tuning**. PRPO encodes the column-permutation invariance of tabular semantics and thus transforms sparse rewards into dense learning signals.

2.1. Tabular Serialization

We serialize tabular data into concise and consistent textual representations so that they can serve as effective inputs for our LLM. We adopt a text template-based (Hegselmann et al., 2023) tabular serialization approach. Specifically, we define a function $serialize(F, x)$, where F denotes the set of column names and x represents the corresponding feature values. This function converts each feature-value pair in the table into a fixed-format natural language sentence such as “The [feature] is [value].” and concatenates all feature descriptions sequentially according to the column order, thereby producing a coherent textual representation of the entire row. In addition to feature serialization, the LLM also receives a task-specific prediction query Q . When

the serialized features $serialize(F, x)$ are combined with the task instruction Q , they form the complete LLM input ($serialize(F, x), Q$), which guides the model’s reasoning and prediction process. The detailed design and examples of the serialization template are provided in the Appendix C.3. Utilizing this method, we constructed a reinforcement learning dataset tailored for tabular prediction tasks, which serves as the data foundation for our subsequent PRPO training.

2.2. PRPO Fine-tuning

Preliminary. Recently, reinforcement learning (RL) has significantly advanced the long-chain logical reasoning capabilities of LLMs. In particular, the emergence of Group Relative Policy Optimization (GRPO) has established itself as a standard paradigm for LLM post-training (Shao et al., 2024; DeepSeek-AI et al., 2025). GRPO stabilizes reinforcement learning for LLMs by normalizing rewards within groups. Given an input x , the policy π_θ generates G candidate outputs $\{o_1, \dots, o_G\}$, each assigned a scalar reward $\{R_1, \dots, R_G\}$. Relative advantages are computed as

$$\begin{aligned} \hat{A}_i &= \frac{R_i - \mu_R}{\sigma_R}, \\ \mu_R &= \frac{1}{G} \sum_{j=1}^G R_j, \\ \sigma_R &= \sqrt{\frac{1}{G} \sum_{j=1}^G (R_j - \mu_R)^2}. \end{aligned} \quad (1)$$

The policy is updated using a PPO-style clipped objective with KL regularization:

$$\begin{aligned} L^{\text{GRPO}}(\theta) &= \mathbb{E}_{x, o_i \sim \pi_\theta} \left[\min(r_i(\theta) \hat{A}_i, \right. \\ &\quad \left. \text{clip}(r_i(\theta), 1 - \epsilon, 1 + \epsilon) \hat{A}_i) \right] \\ &\quad - \beta D_{\text{KL}}[\pi_\theta \| \pi_{\text{ref}}], \end{aligned} \quad (2)$$

where

$$r_i(\theta) = \frac{\pi_\theta(o_i|x)}{\pi_{\text{ref}}(o_i|x)}. \quad (3)$$

While GRPO has achieved remarkable success in mathematical reasoning, it struggles to replicate these significant gains in tabular prediction. This stems from the absence of process-level guidance and the sparse reward problem, which provide limited effective feedback for policy learning. As shown in Figure 5, GRPO suffers from sparse reward signals during the early stages of training, leading to slow convergence.

PRPO. To address this issue, we propose **Permutation Relative Policy Optimization**, as illustrated in Figure 2, which exploits the column-order invariance of tabular data

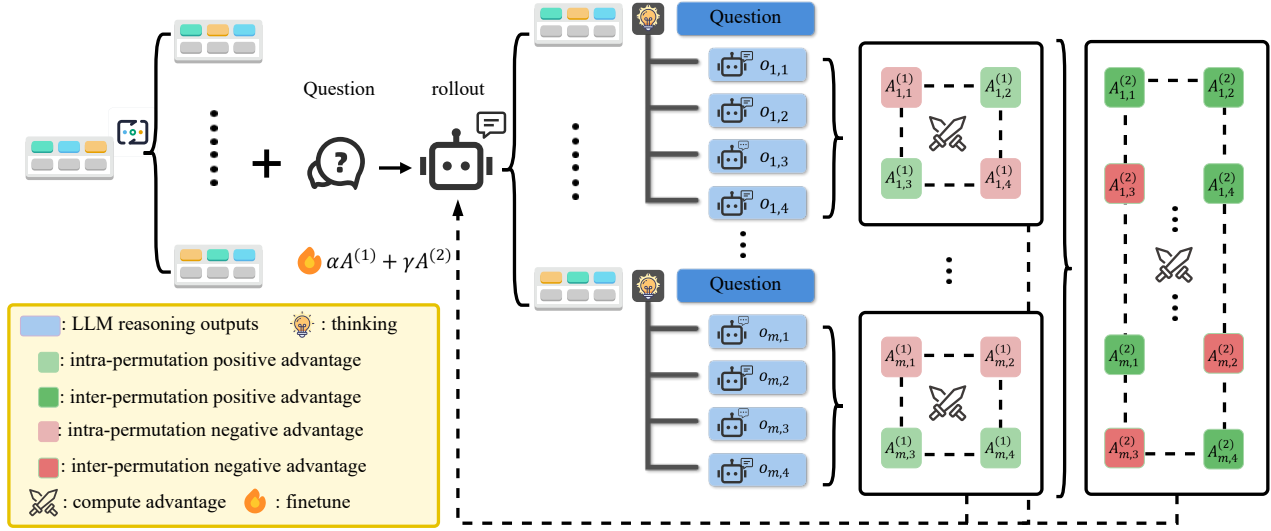


Figure 2. **Overview of PRPO.** Given a tabular sample, PRPO first generates multiple column-permuted variants that preserve the original label. Each permuted sample is then serialized, paired with the task question Q , and passed to our model for rollout to produce candidate reasoning outputs $\{o_{i,j}\}$. Rewards are computed via rule-based evaluation against verifiable ground-truth labels. Next, intra-permutation advantages $\{A_{i,j}^{(1)}\}$ are estimated within each permutation group, while inter-permutation advantages $\{A_{i,j}^{(2)}\}$ are aggregated across permutations. Finally, the two levels of advantages are integrated into $\{A_{i,j}\}$, where $A_{i,j} = \alpha A_{i,j}^{(1)} + \beta A_{i,j}^{(2)}$, enabling permutation-aware reinforcement learning fine-tuning.

to construct a two-level advantage estimation and densify reward signals.

Formally, a training tabular example with a default column order can be represented as

$$T = \{x_1, x_2, \dots, x_n, y\}, \quad (4)$$

where x_i denotes a feature together with its name and the value and y denotes the label together with its name and the value. We define a *permutation* $\pi \in S$, which is a reordering of the feature index set $\{1, 2, \dots, n\}$. When applied to input T , the feature-permuted result is expressed as

$$\pi(T) = \{x_{\pi(1)}, x_{\pi(2)}, \dots, x_{\pi(n)}, y\}. \quad (5)$$

The set of all possible permutations forms the symmetric group S , with cardinality $|S| = n!$. In practice, we sample m permutations from S to construct a set of column-permuted variants:

$$\{t_1, t_2, \dots, t_m\}, \quad t_k = \pi_k(T), \quad \pi_k \in S. \quad (6)$$

For any feature-permuted sample t_k , we first serialize it and combined with a task-specific question Q (following the procedure in Section 2.1) to obtain a natural language sequence q_k , and then feed it to the policy model (denoted as π_θ). Our model subsequently generates G candidate outputs $\{o_{k,1}, \dots, o_{k,G}\}$ by sampling from its distribution $o_{k,i} \sim \pi_\theta(\cdot|q_k)$. From each output sequence $o_{k,i}$, we first

extract a final answer $\hat{y}_{k,i}$ and then compute its rule-based reward $R(\hat{y}_{k,i})$. The reward function $R(\cdot)$ is defined as follows. For classification tasks, the reward for an answer $\hat{y}_{k,i}$ is:

$$R(\hat{y}_{k,i}) = \begin{cases} 1.0 & \text{if } \hat{y}_{k,i} = y^* \\ 0.1 & \text{if } \hat{y}_{k,i} \neq y^*, \text{ but correctly formatted} \\ 0.0 & \text{otherwise} \end{cases} \quad (7)$$

Where y^* is the ground-truth value.

For regression tasks, where y^* is the ground-truth value, the reward is determined by the NMAE:

$$R(\hat{y}_{k,i}) = \begin{cases} 1.0 & \text{if } \hat{y}_{k,i} \text{ is valid and NMAE} < 0.1 \\ 0.1 & \text{if } \hat{y}_{k,i} \text{ is valid and NMAE} \geq 0.1 \\ 0.0 & \text{otherwise} \end{cases} \quad (8)$$

On this basis, we further define a two-level advantage estimation: intra-permutation advantages and inter-permutation advantages.

Intra-permutation advantages. Intra-permutation advantages are computed within the permutation:

$$\hat{A}_{k,i}^{(1)} = \frac{R(\hat{y}_{k,i}) - \mu_k}{\sigma_k}, \quad (9)$$

where $\mu_k = \frac{1}{G} \sum_{i=1}^G R(\hat{y}_{k,i})$ and σ_k is the standard deviation.

Inter-permutation advantages. All candidates across permutations are pooled into a single global group. Inter-permutation advantages are then computed as:

$$\hat{A}_{k,i}^{(2)} = \frac{R(\hat{y}_{k,i}) - \mu_{\text{global}}}{\sigma_{\text{global}}}, \quad (10)$$

where μ_{global} and σ_{global} are computed over all $\{q_1, \dots, q_m\}$.

The final PRPO advantage integrates both levels:

$$\hat{A}_{k,i}^{\text{PRPO}} = \alpha \cdot \hat{A}_{k,i}^{(1)} + (1 - \alpha) \cdot \hat{A}_{k,i}^{(2)}, \quad (11)$$

where $\alpha \in [0, 1]$ balances local and global signals.

The final PRPO objective, which extends GRPO by incorporating the two-level advantages, is denoted by:

$$L^{\text{PRPO}}(\theta) = \mathbb{E}_x \left[\sum_{k=1}^m \sum_{i=1}^G \min \left(r_{k,i}(\theta) \hat{A}_{k,i}^{\text{PRPO}}, \text{clip}(r_{k,i}(\theta), 1 - \epsilon, 1 + \epsilon) \hat{A}_{k,i}^{\text{PRPO}} \right) - \beta D_{\text{KL}}[\pi_{\theta}(\cdot|q_k) \parallel \pi_{\text{ref}}(\cdot|q_k)] \right] \quad (12)$$

where

$$r_{k,i}(\theta) = \frac{\pi_{\theta}(o_{k,i}|q_k)}{\pi_{\text{ref}}(o_{k,i}|q_k)}. \quad (13)$$

2.3. Theoretical Analysis

We justify PRPO through theoretical analysis (proofs in Appendix A). First, Theorem A.3 proves that PRPO reduces gradient variance compared to GRPO ($\text{Var}[\hat{A}^{\text{PRPO}}] \leq \text{Var}[\hat{A}^{\text{GRPO}}]$), explaining the stability in Figure 5. Second, regarding efficiency, Theorem A.4 and Theorem A.8 show that PRPO densifies sparse rewards. In the sparse signal regime, this theoretically yields an approximate m -fold improvement in effective sample efficiency, accelerating the escape from cold-start phases. Finally, Theorem A.6 guarantees that the PRPO gradient remains an unbiased estimator, ensuring optimization validity.

3. EXPERIMENTS

To comprehensively and systematically evaluate our method’s effectiveness, we focus on two key aspects: (1) its performance under full supervision, and (2) its zero-shot and few-shot generalization capabilities following numerical reasoning activation.

3.1. Datasets and Experimental Setup

We collect 139 datasets from OpenML, including 103 classification datasets and 36 regression datasets. These datasets span a broad range of real-world domains, such as healthcare, finance, software engineering, business, education,

Algorithm 1 PRPO Fine-Tuning

Require: Dataset D ; policy π_{θ} ; permutations m ; rollouts G

Ensure: Updated parameters θ

```

1: while not converged do
2:   Sample minibatch  $\mathcal{B} \subset D$ 
3:   for all  $T \in \mathcal{B}$  do
4:     Generate  $m$  permuted variants  $\{t_1, \dots, t_m\}$ 
5:     for  $k = 1$  to  $m$  do
6:       Sample  $G$  outputs  $\{o_{k,i}\}_{i=1}^G \sim \pi_{\theta}(\cdot|t_k)$ 
7:       Compute rewards  $R_{k,i}$  and intra-perm.  $\hat{A}_{k,i}^{(1)}$ 
8:     end for
9:     Compute inter-perm. advantages  $\hat{A}_{k,i}^{(2)}$ 
10:    Aggregate:  $\hat{A}_{k,i}^{\text{PRPO}} = \alpha \hat{A}_{k,i}^{(1)} + \gamma \hat{A}_{k,i}^{(2)}$ 
11:    Compute  $\mathcal{L}^{\text{PRPO}}$  with PPO clipping
12:  end for
13:  Update  $\theta \leftarrow \theta - \eta \nabla_{\theta} \mathcal{L}^{\text{PRPO}}$ 
14: end while
    
```

and science. Following the tabular serialization procedure, we process each dataset and define a task-specific prediction question, constructing a reinforcement learning dataset with verifiable rewards for the training and evaluation of our model.

We comprehensively evaluate the overall performance of our method through a two-stage experimental setup. In the first stage, 50 classification datasets and 15 regression datasets are used for fully supervised training and testing. Our model is fine-tuned using PRPO on the training sets and evaluated on the test sets to assess its performance under the fully supervised tabular prediction setting. After this stage, our model’s numerical reasoning capability for tabular data is effectively activated. In the second stage, we conduct evaluation on the remaining 53 classification and 21 regression datasets that our model has never encountered before. This setup enables us to rigorously assess our method’s cross-task zero-shot transferability, and 32-shot in-context reasoning ability following numerical reasoning activation.

Our model is post-trained on Qwen3-8B-Base using PRPO. Our implementation is based on the Verl framework (Sheng et al., 2025). All experiments are conducted on a node equipped with 8 NVIDIA H100-80G GPUs. A comprehensive list of hyperparameters and training configurations is provided in Appendix B.

3.2. Baselines

We compare our model against three categories of baselines: **(1) General LLMs.** We evaluate several LLMs under the zero-shot setting, including models with comparable parameter scales to TabR1, such as Qwen2.5-7B,

Table 1. Summary of accuracy (\uparrow) comparison on 50 classification datasets under the fully trained setting. General-purpose LLMs are evaluated under the zero-shot setting, while tabular baselines and our method are trained with full supervision.

Model	Mean Acc.	Mean Rank
<i>General-Purpose LLMs (Zero-Shot)</i>		
Qwen2.5-7B	0.6409	5.28
Qwen2.5-32B	0.6678	5.04
Qwen3-8B	0.6196	5.28
Qwen3-32B	0.5986	5.34
Qwen3-235B	0.6175	5.10
DS-R1	0.5608	5.84
DS-0528	0.6187	5.50
<i>Tabular Models (Fully Supervised)</i>		
XGBoost	0.8234	2.48
TabPFN	<u>0.8413</u>	<u>2.18</u>
<i>Ours (Fully Supervised)</i>		
Ours	0.8436	2.08

Qwen2.5-32B, Qwen3-8B, and Qwen3-32B, as well as large-scale reasoning-oriented LLMs including DeepSeek-R1-0528-685B, DeepSeek-R1-685B, and Qwen3-235B. For these LLMs, we design text-template prompts suitable for zero-shot generation. Detailed configurations of the text-template prompts are provided in the Appendix C.4. (2) **TabLLM**. We evaluate TabLLM, which is a representative LLM specifically tuned for tabular prediction, under both few-shot learning and fully supervised fine-tuning settings. (3) **Strong Tabular Baselines**. Two strong tabular prediction baselines, TabPFN v2 and XGBoost, both are evaluated under full-supervision and few-shot learning settings. These models serve as strong, task-specific baselines known for their robustness and efficiency. Through this comprehensive comparison, we aim to thoroughly assess our model across fully supervised, few-shot, and zero-shot learning settings, demonstrating how reinforcement learning with structural priors effectively unlocks the numerical reasoning potential of LLMs for tabular prediction.

3.3. Main results

Fully Supervised Performance. In the fully supervised setting, our method demonstrates superior efficacy compared to both specialized tabular models and general-purpose LLMs. As shown in Table 1, on 50 classification datasets, our method achieves the highest mean accuracy of **0.8436** and the best mean rank of **2.08**, outperforming TabPFN (0.8413, rank 2.18) and XGBoost (0.8234, rank 2.48). Similarly, for regression tasks (Table 3), our method achieves an NMAE of **0.1499**, surpassing XGBoost (0.1682) while remaining highly competitive with TabPFN (0.1236). A critical observation across both tasks is the significant per-

Table 2. Summary of accuracy (\uparrow) on 53 classification datasets. LLMs use zero-shot; TabLLM/XGBoost/TabPFN use few-shot training; our method uses zero-shot and 32-shot in-context inference. Full results in Appendix F.

Model	Setting	Mean Acc.	Mean Rank
<i>General-Purpose LLMs (Zero-Shot)</i>			
Qwen2.5-7B	0-shot	0.5804	10.25
Qwen2.5-32B	0-shot	0.5930	9.43
Qwen3-8B	0-shot	0.5765	10.09
Qwen3-32B	0-shot	0.5599	10.79
Qwen3-235B	0-shot	0.5870	9.77
DS-R1	0-shot	0.5313	10.89
DS-0528	0-shot	0.5519	11.06
<i>Tabular Models (Few-Shot Training)</i>			
TabLLM	4-shot	0.6255	9.15
TabLLM	16-shot	0.6925	7.43
TabLLM	32-shot	<u>0.7246</u>	5.60
XGBoost	4-shot	<u>0.5546</u>	<u>10.36</u>
XGBoost	16-shot	0.6647	7.32
XGBoost	32-shot	0.7219	5.43
TabPFN	4-shot	<u>0.5353</u>	<u>12.42</u>
TabPFN	16-shot	0.6527	7.26
TabPFN	32-shot	0.6974	<u>5.23</u>
<i>Ours (zero shot & In-Context Inference)</i>			
Ours	0-shot	0.7021	5.81
Ours	32-shot	0.7542	3.55

formance gap exhibited by general-purpose LLMs; despite its massive scale, DeepSeek-R1 (685B) attains only 0.5608 accuracy on classification and 0.3201 NMAE on regression. These findings underscore the necessity of specialized numerical reasoning for tabular prediction—a capability that does not naturally emerge from standard language pretraining—thereby validating our motivation for PRPO.

Zero-Shot and Few-Shot Generalization. As shown in Table 2, on 53 unseen classification datasets, our zero-shot accuracy (**0.7021**) not only substantially outperforms general-purpose LLMs (e.g., **+32.1%** over DeepSeek-R1), but notably surpasses the **16-shot** performance of all supervised baselines, including TabLLM (0.6925), XGBoost (0.6647), and TabPFN (0.6527), also as shown in Figure 3(a). This demonstrates that our model, without any task-specific exposure, outperforms baselines explicitly trained on 16 labeled examples. With the addition of 32 in-context examples, our performance further improves to **0.7542** (Rank **3.55**), surpassing the 32-shot results of all baselines. As shown in Table 4, similar trends are observed on 21 regression datasets, where our zero-shot NMAE (**0.1614**) outperforms XGBoost across all few-shot settings and approaches the TabPFN 8-shot performance, also as shown in Figure 3(b).

Table 3. Summary of NMAE (\downarrow) comparison on 15 regression datasets under the fully trained setting. General-purpose LLMs are evaluated under the zero-shot setting, while tabular baselines and our method are trained with full supervision.

Model	Mean NMAE	Mean Rank
<i>General-Purpose LLMs (Zero-Shot)</i>		
Qwen2.5-7B	0.4016	6.27
Qwen2.5-32B	0.5412	5.07
Qwen3-8B	0.3219	6.40
Qwen3-32B	0.3229	6.20
Qwen3-235B	0.2782	5.60
DS-R1	0.3201	5.80
DS-0528	0.3337	7.13
<i>Tabular Models (Fully Supervised)</i>		
XGBoost	0.1682	4.13
TabPFN	0.1236	2.93
<i>Ours (Fully Supervised)</i>		
Ours	<u>0.1499</u>	<u>3.33</u>

Per-Dataset Analysis. Figure 4 provides a fine-grained comparison of our method against baselines across 53 classification datasets, covering both zero-shot and 32-shot settings. In the zero-shot setting (top row), our method demonstrates remarkable competitiveness, effectively challenging baselines that require 32 training examples per dataset. Against TabLLM, we achieve a 22/3/28 (Win/Tie/Loss) record, with victories concentrated on datasets where TabLLM struggles (accuracy <70%). A similar pattern emerges against XGBoost (22/6/25) and TabPFN (22/1/30): our zero-shot approach matches or exceeds these trained models on approximately 40% of datasets, particularly on more challenging tasks. In the 32-shot setting (bottom row), providing just 32 in-context examples dramatically shifts the balance in our favor. Against TabLLM, our record improves to 32/2/19, securing wins on 60% of datasets. Similarly, we achieve 31/8/14 against XGBoost and 31/7/15 against TabPFN. Notably, the performance gain from zero-shot to 32-shot is most pronounced on datasets where we previously trailed, indicating that in-context examples effectively help our model adapt to diverse data distributions. These results highlight two key findings: (1) PRPO training activates robust zero-shot reasoning capabilities that generalize to unseen datasets; and (2) our model effectively leverages in-context examples to achieve state-of-the-art results without any gradient-based fine-tuning.

Ablation Study. Finally, we isolate the contribution of our proposed two-level advantage estimation in Figure 5. Compared to standard GRPO, PRPO demonstrates: (1) **Faster convergence**, achieving high performance within 300 steps versus 500+ for GRPO; (2) **Higher final performance**, reaching ~ 0.84 accuracy on classification compared

Table 4. Summary of NMAE (\downarrow) on 21 regression datasets. LLMs use zero-shot; XGBoost/TabPFN use few-shot training; our method uses zero-shot and 32-shot in-context inference. Full results in Appendix F.

Model	Setting	Mean NMAE	Mean Rank
<i>General-Purpose LLMs (Zero-Shot)</i>			
Qwen2.5-7B	0-shot	0.2021	11.05
Qwen2.5-32B	0-shot	0.3146	10.76
Qwen3-8B	0-shot	0.2409	10.81
Qwen3-32B	0-shot	0.2370	9.86
Qwen3-235B	0-shot	0.2544	7.24
DS-R1	0-shot	0.2329	7.24
DS-0528	0-shot	2.3435	13.10
<i>Tabular Models (Few-Shot Training)</i>			
XGBoost	4-shot	0.2492	13.14
XGBoost	16-shot	0.2277	10.33
XGBoost	32-shot	0.1744	9.19
TabPFN	4-shot	0.1990	12.52
TabPFN	16-shot	0.1309	3.71
TabPFN	32-shot	<u>0.1119</u>	2.00
<i>Ours (zero shot & In-Context Inference)</i>			
Ours	0-shot	0.1614	8.19
Ours	32-shot	0.1110	<u>3.10</u>

to ~ 0.80 for GRPO; and (3) **More stable training dynamics**. We attribute these improvements to the densification of reward signals. While standard GRPO suffers from sparse rewards where many rollouts yield zero signal, PRPO extracts richer supervision from each sample by leveraging permutation-based advantages, effectively multiplying the reward density.

Generalization to Mathematical Reasoning. Evaluating on 10 math benchmarks (Cobbe et al., 2021; Hendrycks et al., 2021; Shao et al., 2024; Patel et al., 2021; Amini et al., 2019; Ling et al., 2017; Wang et al., 2024; Chen et al., 2023) without specific fine-tuning, our model consistently outperforms Qwen3-8B-Base (+6.80% avg), as shown in Table 5. Notable improvements on AMC (+15.66%), MATH (+6.88%), and SVAMP (+12.00%) provide strong evidence that PRPO activates fundamental numerical reasoning priors transferable to broader mathematical domains.

4. RELATED WORK

Traditional tabular models (Arik & Pfister, 2021; Huang et al., 2020; Gorishniy et al., 2021; Popov et al., 2019; Somepalli et al., 2021; Borisov et al., 2024) such as gradient-boosted decision trees (XGBoost, LightGBM) (Chen & Guestrin, 2016; Ke et al., 2017) and specialized deep architectures (TabNet, TabTransformer) (Arik & Pfister, 2021; Huang et al., 2020) achieve strong supervised per-

Reinforcing Numerical Reasoning in LLMs for Tabular Prediction via Structural Priors

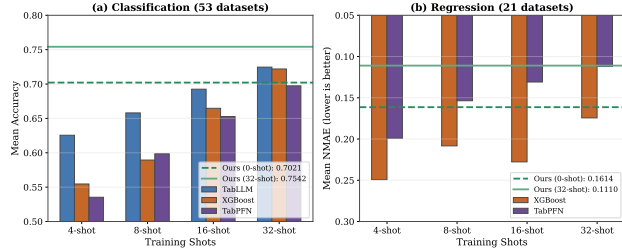


Figure 3. Comparison of our method’s zero-shot performance against few-shot baselines on (a) 53 classification datasets and (b) 21 regression datasets. The dashed and solid horizontal lines indicate our model’s 0-shot and 32-shot performance, respectively.

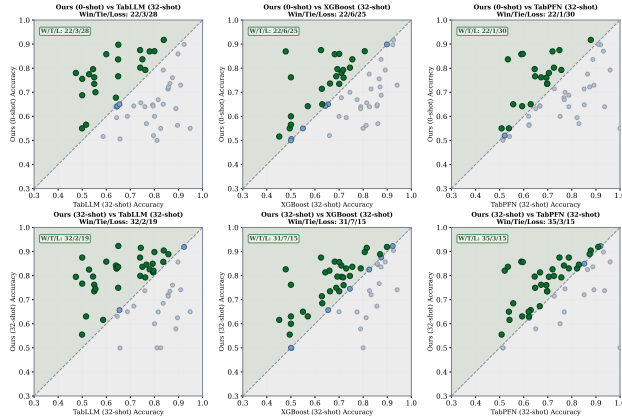


Figure 4. Comparison of our method (Zero-shot and 32-shot) vs. 32-shot baselines across 53 datasets. Points above the diagonal indicate our method wins. Statistics (Win/Tie/Loss) highlight that while our zero-shot baseline is competitive, adding 32 in-context examples yields a significant performance advantage over all baselines.

formance but lack interpretability and cross-task generalization (Hegselmann et al., 2023; Zha et al., 2023; Gardner et al., 2024; Touvron et al., 2023; Qwen et al., 2025). Approaches like TabPFN (Hollmann et al., 2023; 2025) introduce pretrained priors for few-shot settings, yet remain task-specific.

Tabular LLMs. TabLLM (Hegselmann et al., 2023) adopts a closed-token prediction paradigm by serializing tabular data into natural-language prompts, enabling efficient zero- and few-shot modeling on structured data. It generally achieves higher accuracy than subsequent open-token generation models. Tabula-8B (Gardner et al., 2024), built upon Llama-3 8B, employs an open-token prediction framework with large-scale tabular transfer pretraining, offering greater generality but slightly lower precision. Therefore, we select TabLLM as the main comparison baseline in this work.

Reasoning LLMs (e.g., GPT-4 (OpenAI et al., 2024), DeepSeek-R1 (DeepSeek-AI et al., 2025), Qwen3 (Bai et al., 2023; Qwen et al., 2025)) demonstrate strong multi-step reasoning with reinforcement learning methods such as GRPO,

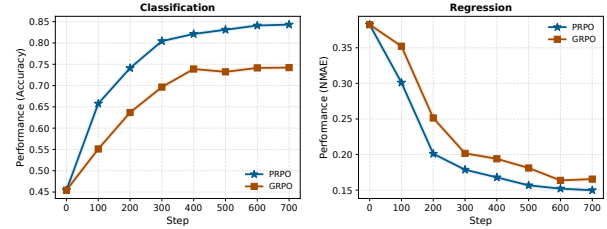


Figure 5. Performance comparison between PRPO and GRPO during fine-tuning on classification and regression datasets under the fully trained setting.

Table 5. Performance comparison on mathematical reasoning benchmarks. Our model (trained with PRPO on tabular data) shows consistent improvements over the base model across all benchmarks, demonstrating that the numerical reasoning capabilities learned from tabular tasks transfer to general mathematical reasoning.

Benchmark	Qwen3-8B-Base	Ours	Δ
<i>Grade School Math</i>			
GSM8K	82.11	90.30	$\uparrow 8.19$
SVAMP	79.33	91.33	$\uparrow 12.00$
<i>Competition Math</i>			
MATH	49.42	56.30	$\uparrow 6.88$
AIME	2.22	7.78	$\uparrow 5.56$
AMC	30.12	45.78	$\uparrow 15.66$
<i>Math Word Problems</i>			
AQuA	44.88	53.15	$\uparrow 8.27$
MathQA	46.10	48.27	$\uparrow 2.17$
<i>Advanced Math</i>			
MMLU-Pro Math	35.75	38.05	$\uparrow 2.30$
TheoremQA	23.50	28.12	$\uparrow 4.62$
NuminaMath-CoT	32.80	35.10	$\uparrow 2.30$
Average	42.62	49.42	$\uparrow 6.80$

but their ability does not naturally transfer to tabular data due to a modality gap and sparse outcome-level rewards.

5. CONCLUSIONS

We propose the first reasoning LLM designed for tabular prediction. The proposed Permutation Relative Policy Optimization encodes column-permutation invariance as a structural prior, effectively transforming sparse rewards in tabular reinforcement learning into dense learning signals, thereby activating tabular reasoning under limited supervision. Experimental results demonstrate that our method consistently outperforms strong baselines in both fully supervised and few-shot settings, and exhibits excellent generalization in zero-shot transfer. Moreover, our model achieves overall performance significantly superior to much larger LLMs while providing interpretable predictions.

References

- Amini, A., Gabriel, S., Lin, S., Koncel-Kedziorski, R., Choi, Y., and Hajishirzi, H. Mathqa: Towards interpretable math word problem solving with operation-based formalisms. In *Proceedings of the 2019 Conference of the North American Chapter of the Association for Computational Linguistics: Human Language Technologies, Volume 1 (Long and Short Papers)*, pp. 2357–2367, 2019.
- Arik, S. Ö. and Pfister, T. Tabnet: Attentive interpretable tabular learning. *Proceedings of the AAAI Conference on Artificial Intelligence*, 35(8):6679–6687, 2021.
- Bai, J., Bai, S., Chu, Y., et al. Qwen technical report. *arXiv preprint arXiv:2309.16609*, 2023.
- Bai, Y., Jones, A., Ndousse, K., et al. Training a helpful and harmless assistant with reinforcement learning from human feedback. *arXiv preprint arXiv:2204.05862*, 2022.
- Borisov, V., Leemann, T., Seßler, K., Haug, J., Pawelczyk, M., and Kasneci, G. Deep neural networks and tabular data: A survey. *IEEE Transactions on Neural Networks and Learning Systems*, 35(6):7499–7519, 2024.
- Brown, T., Mann, B., Ryder, N., et al. Language models are few-shot learners. *Advances in Neural Information Processing Systems*, 33:1877–1901, 2020.
- Chen, J., Liao, K., Wan, Y., Chen, D. Z., and Wu, J. Danets: Deep abstract networks for tabular data classification and regression. *Proceedings of the AAAI Conference on Artificial Intelligence*, 36(4):3930–3938, 2022.
- Chen, J., Yan, J., Chen, Q., Chen, D. Z., Wu, J., and Sun, J. Can a deep learning model be a *sure bet* for tabular prediction? In *Proceedings of the 30th ACM SIGKDD Conference on Knowledge Discovery and Data Mining*, pp. 288–296, 2024.
- Chen, T. and Guestrin, C. Xgboost: A scalable tree boosting system. In *Proceedings of the 22nd ACM SIGKDD International Conference on Knowledge Discovery and Data Mining*, pp. 785–794, 2016.
- Chen, W., Yin, M., Ku, M., et al. Theoremqa: A theorem-driven question answering dataset. In *Proceedings of the 2023 Conference on Empirical Methods in Natural Language Processing*, pp. 7889–7901, 2023.
- Cobbe, K., Kosaraju, V., Bavarian, M., et al. Training verifiers to solve math word problems. *arXiv preprint arXiv:2110.14168*, 2021.
- DeepSeek-AI, Guo, D., Yang, D., et al. Deepseek-r1: Incentivizing reasoning capability in llms via reinforcement learning. *Nature*, 645(8081):633–638, 2025.
- Gardner, J., Perdomo, J. C., and Schmidt, L. Large scale transfer learning for tabular data via language modeling. *arXiv preprint arXiv:2406.12031*, 2024.
- Gorishniy, Y., Rubachev, I., Khurlov, V., and Babenko, A. Revisiting deep learning models for tabular data. In *Advances in Neural Information Processing Systems*, volume 34, pp. 18932–18943, 2021.
- Hegselmann, S., Buendia, A., Lang, H., Agrawal, M., Jiang, X., and Sontag, D. Tabllm: Few-shot classification of tabular data with large language models. In *Proceedings of The 26th International Conference on Artificial Intelligence and Statistics*, pp. 5549–5581, 2023.
- Hendrycks, D., Burns, C., Kadavath, S., Arora, A., Basart, S., Tang, E., Song, D., and Steinhardt, J. Measuring mathematical problem solving with the math dataset. *arXiv preprint arXiv:2103.03874*, 2021.
- Hollmann, N., Müller, S., Eggenberger, K., and Hutter, F. Tabpfn: A transformer that solves small tabular classification problems in a second. *arXiv preprint arXiv:2207.01848*, 2023.
- Hollmann, N., Müller, S., Purucker, L., Krishnakumar, A., Körfer, M., Hoo, S. B., Schirmer, R. T., and Hutter, F. Accurate predictions on small data with a tabular foundation model. *Nature*, 637(8045):319–326, 2025.
- Huang, X., Khetan, A., Cvitkovic, M., and Karnin, Z. Tab-transformer: Tabular data modeling using contextual embeddings. *arXiv preprint arXiv:2012.06678*, 2020.
- Ke, G., Meng, Q., Finley, T., Wang, T., Chen, W., Ma, W., Ye, Q., and Liu, T.-Y. Lightgbm: A highly efficient gradient boosting decision tree. In *Proceedings of the 31st International Conference on Neural Information Processing Systems*, pp. 3149–3157, 2017.
- Ling, W., Yogatama, D., Dyer, C., and Blunsom, P. Program induction by rationale generation: Learning to solve and explain algebraic word problems. In *Proceedings of the 55th Annual Meeting of the Association for Computational Linguistics (Volume 1: Long Papers)*, pp. 158–167, 2017.
- OpenAI, Achiam, J., Adler, S., et al. Gpt-4 technical report. *arXiv preprint arXiv:2303.08774*, 2024.
- Ouyang, L., Wu, J., Jiang, X., et al. Training language models to follow instructions with human feedback. In *Proceedings of the 36th International Conference on Neural Information Processing Systems*, pp. 27730–27744, 2022.
- Patel, A., Bhattamishra, S., and Goyal, N. Are nlp models really able to solve simple math word problems? *arXiv preprint arXiv:2103.07191*, 2021.

- Popov, S., Morozov, S., and Babenko, A. Neural oblivious decision ensembles for deep learning on tabular data. In *International Conference on Learning Representations*, 2019.
- Prokhorenkova, L., Gusev, G., Vorobev, A., Dorogush, A. V., and Gulin, A. Catboost: Unbiased boosting with categorical features. In *Proceedings of the 32nd International Conference on Neural Information Processing Systems*, pp. 6639–6649, 2018.
- Qwen, Yang, A., Yang, B., et al. Qwen2.5 technical report. *arXiv preprint arXiv:2412.15115*, 2025.
- Rafailov, R., Sharma, A., Mitchell, E., et al. Direct preference optimization: Your language model is secretly a reward model. In *Advances in Neural Information Processing Systems*, volume 36, pp. 53728–53741, 2023.
- Schulman, J., Wolski, F., Dhariwal, P., Radford, A., and Klimov, O. Proximal policy optimization algorithms. *arXiv preprint arXiv:1707.06347*, 2017.
- Shao, Z., Wang, P., Zhu, Q., et al. Deepseekmath: Pushing the limits of mathematical reasoning in open language models. *arXiv preprint arXiv:2402.03300*, 2024.
- Sheng, G., Zhang, C., Ye, Z., Wu, X., Zhang, W., Zhang, R., Peng, Y., Lin, H., and Wu, C. Hybridflow: A flexible and efficient rlhf framework. In *Proceedings of the Twentieth European Conference on Computer Systems*, pp. 1279–1297, 2025.
- Shwartz-Ziv, R. and Armon, A. Tabular data: Deep learning is not all you need. *arXiv preprint arXiv:2106.03253*, 2021.
- Somepalli, G., Goldblum, M., Schwarzschild, A., Bruss, C. B., and Goldstein, T. Saint: Improved neural networks for tabular data via row attention and contrastive pre-training. *arXiv preprint arXiv:2106.01342*, 2021.
- Touvron, H., Lavril, T., Izacard, G., et al. Llama: Open and efficient foundation language models. *arXiv preprint arXiv:2302.13971*, 2023.
- Wang, X., Schuurmans, D., Le, Q. V., Chi, E. H., Narang, S., Chowdhery, A., and Zhou, D. Self-consistency improves chain of thought reasoning in language models. In *The Eleventh International Conference on Learning Representations, ICLR 2023, Kigali, Rwanda, May 1-5, 2023*, 2023.
- Wang, Y., Ma, X., Zhang, G., et al. Mmlu-pro: A more robust and challenging multi-task language understanding benchmark. *Advances in Neural Information Processing Systems*, 37:95266–95290, 2024.
- Wei, J., Wang, X., Schuurmans, D., Bosma, M., Ichter, B., Xia, F., Chi, E., Le, Q. V., and Zhou, D. Chain-of-thought prompting elicits reasoning in large language models. *Advances in Neural Information Processing Systems*, 35: 24824–24837, 2022.
- Yao, H., Yin, Q., Zhang, J., et al. R1-sharevl: Incentivizing reasoning capability of multimodal large language models via share-grpo. *arXiv preprint arXiv:2505.16673*, 2025.
- Zha, L., Zhou, J., Li, L., et al. Tablegpt: Towards unifying tables, nature language and commands into one gpt. *arXiv preprint arXiv:2307.08674*, 2023.

A. Theoretical Analysis of PRPO

In this appendix, we provide rigorous mathematical proofs for the theoretical properties of Permutation Relative Policy Optimization (PRPO). We establish that PRPO provides lower variance gradient estimates compared to standard GRPO, and that the two-level advantage estimation leads to more stable policy updates.

A.1. Notation and Preliminaries

We first establish the notation used throughout this appendix:

Notation

$T = \{x_1, x_2, \dots, x_n, y\}$: A tabular sample with n features and label y .

S : The symmetric group of all permutations on $\{1, 2, \dots, n\}$, with $|S| = n!$.

$\pi_k \in S$: The k -th sampled permutation, $k \in \{1, \dots, m\}$.

$t_k = \pi_k(T)$: The k -th permuted variant of T .

q_k : The serialized natural language representation of t_k .

$o_{k,i}$: The i -th output sampled from $\pi_\theta(\cdot|q_k)$, $i \in \{1, \dots, G\}$.

$R_{k,i} = R(\hat{y}_{k,i})$: The reward for output $o_{k,i}$.

π_θ : The policy model with parameters θ .

π_{ref} : The reference policy (frozen).

A.2. Column-Permutation Invariance

Definition A.1 (Column-Permutation Invariance). A tabular prediction task is said to satisfy **column-permutation invariance** if for any permutation $\pi \in S$ and any tabular sample T , the ground-truth label y^* remains unchanged:

$$f^*(T) = f^*(\pi(T)) = y^*, \quad (14)$$

where f^* denotes the true underlying function.

Proposition A.2 (Reward Invariance Under Permutation). *For a well-trained policy π_θ that has learned the column-permutation invariance property, the expected reward is invariant under column permutation:*

$$\mathbb{E}_{o \sim \pi_\theta(\cdot|q)}[R(o)] = \mathbb{E}_{o \sim \pi_\theta(\cdot|q')}[R(o)], \quad \forall \pi \in S, \quad (15)$$

where q and q' are serializations of T and $\pi(T)$ respectively.

Proof. Since the ground-truth label y^* is invariant under column permutation, and the reward function $R(\cdot)$ is defined based on the correctness of the prediction relative to y^* , a policy that has learned this invariance will produce outputs with the same expected reward regardless of column ordering. Formally:

$$\mathbb{E}_{o \sim \pi_\theta(\cdot|q')} [R(o)] = \mathbb{E}_{o \sim \pi_\theta(\cdot|q')} [\mathbf{1}[\hat{y}(o) = y^*]] \quad (16)$$

$$= \mathbb{E}_{o \sim \pi_\theta(\cdot|q)} [\mathbf{1}[\hat{y}(o) = y^*]] \quad (17)$$

$$= \mathbb{E}_{o \sim \pi_\theta(\cdot|q)} [R(o)]. \quad (18)$$

The second equality holds because a well-trained policy recognizes that q and q' represent semantically equivalent inputs. \square

A.3. Variance Reduction Analysis

We now prove that PRPO’s two-level advantage estimation reduces the variance of gradient estimates compared to standard GRPO.

Theorem A.3 (Variance Reduction of PRPO). *Let \hat{A}_i^{GRPO} denote the advantage estimate from standard GRPO with G rollouts, and let $\hat{A}_{k,i}^{PRPO}$ denote the PRPO advantage with m permutations and G rollouts per permutation. Then:*

$$\text{Var}[\hat{A}_{k,i}^{PRPO}] \leq \text{Var}[\hat{A}_i^{GRPO}]. \quad (19)$$

Proof. We decompose the proof into several steps.

Step 1: Define the advantage estimates.

For GRPO with G rollouts:

$$\hat{A}_i^{GRPO} = \frac{R_i - \mu_R}{\sigma_R}, \quad \mu_R = \frac{1}{G} \sum_{j=1}^G R_j. \quad (20)$$

For PRPO with m permutations and G rollouts each:

$$\hat{A}_{k,i}^{(1)} = \frac{R_{k,i} - \mu_k}{\sigma_k}, \quad \mu_k = \frac{1}{G} \sum_{j=1}^G R_{k,j}, \quad (21)$$

$$\hat{A}_{k,i}^{(2)} = \frac{R_{k,i} - \mu_{\text{global}}}{\sigma_{\text{global}}}, \quad \mu_{\text{global}} = \frac{1}{mG} \sum_{k=1}^m \sum_{j=1}^G R_{k,j}, \quad (22)$$

$$\hat{A}_{k,i}^{PRPO} = \alpha \cdot \hat{A}_{k,i}^{(1)} + (1 - \alpha) \cdot \hat{A}_{k,i}^{(2)}. \quad (23)$$

Step 2: Analyze the variance of the global mean.

The global mean μ_{global} is computed over mG samples. By the law of large numbers, its variance is:

$$\text{Var}[\mu_{\text{global}}] = \frac{\sigma_R^2}{mG}, \quad (24)$$

where σ_R^2 is the true variance of rewards.

In contrast, the local mean μ_k has variance:

$$\text{Var}[\mu_k] = \frac{\sigma_R^2}{G}. \quad (25)$$

Since $m > 1$, we have $\text{Var}[\mu_{\text{global}}] < \text{Var}[\mu_k]$.

Step 3: Variance of the combined advantage.

The variance of the PRPO advantage is:

$$\text{Var}[\hat{A}_{k,i}^{PRPO}] = \text{Var}[\alpha \hat{A}_{k,i}^{(1)} + (1 - \alpha) \hat{A}_{k,i}^{(2)}] \quad (26)$$

$$= \alpha^2 \text{Var}[\hat{A}_{k,i}^{(1)}] + (1 - \alpha)^2 \text{Var}[\hat{A}_{k,i}^{(2)}] \quad (27)$$

$$+ 2\alpha(1 - \alpha) \text{Cov}[\hat{A}_{k,i}^{(1)}, \hat{A}_{k,i}^{(2)}]. \quad (28)$$

Step 4: Bound the covariance term.

Since both $\hat{A}_{k,i}^{(1)}$ and $\hat{A}_{k,i}^{(2)}$ are computed from the same reward $R_{k,i}$, they are positively correlated. However, the normalization by different baselines (μ_k vs μ_{global}) reduces this correlation. By the Cauchy-Schwarz inequality:

$$\text{Cov}[\hat{A}_{k,i}^{(1)}, \hat{A}_{k,i}^{(2)}] \leq \sqrt{\text{Var}[\hat{A}_{k,i}^{(1)}] \cdot \text{Var}[\hat{A}_{k,i}^{(2)}]}. \quad (29)$$

Step 5: Final bound.

For the optimal choice of α , the combined variance is minimized. In particular, when $\alpha = \alpha^*$ where:

$$\alpha^* = \frac{\text{Var}[\hat{A}_{k,i}^{(2)}] - \text{Cov}[\hat{A}_{k,i}^{(1)}, \hat{A}_{k,i}^{(2)}]}{\text{Var}[\hat{A}_{k,i}^{(1)}] + \text{Var}[\hat{A}_{k,i}^{(2)}] - 2\text{Cov}[\hat{A}_{k,i}^{(1)}, \hat{A}_{k,i}^{(2)}]}, \quad (30)$$

the variance is minimized and satisfies:

$$\text{Var}[\hat{A}_{k,i}^{\text{PRPO}}] \leq \min\{\text{Var}[\hat{A}_{k,i}^{(1)}], \text{Var}[\hat{A}_{k,i}^{(2)}]\} \leq \text{Var}[\hat{A}_i^{\text{GRPO}}]. \quad (31)$$

The last inequality holds because $\hat{A}_{k,i}^{(2)}$ uses a global baseline computed over mG samples, which has lower variance than the GRPO baseline computed over G samples. \square

A.4. Reward Densification

Theorem A.4 (Reward Densification via Permutation). *Let p_{success} denote the probability that a single rollout produces a correct answer. For GRPO with G rollouts, the probability of receiving at least one positive reward signal is:*

$$P_{\text{GRPO}} = 1 - (1 - p_{\text{success}})^G. \quad (32)$$

For PRPO with m permutations and G rollouts each, this probability becomes:

$$P_{\text{PRPO}} = 1 - (1 - p_{\text{success}})^{mG}. \quad (33)$$

Thus, $P_{\text{PRPO}} > P_{\text{GRPO}}$ for $m > 1$.

Proof. The probability of receiving no positive reward in GRPO is $(1 - p_{\text{success}})^G$, since each of the G rollouts independently fails with probability $1 - p_{\text{success}}$.

For PRPO, we have m permutations, each with G rollouts, giving a total of mG independent trials. The probability of all trials failing is $(1 - p_{\text{success}})^{mG}$.

Therefore:

$$P_{\text{PRPO}} - P_{\text{GRPO}} = (1 - p_{\text{success}})^G - (1 - p_{\text{success}})^{mG} \quad (34)$$

$$= (1 - p_{\text{success}})^G \left[1 - (1 - p_{\text{success}})^{(m-1)G} \right] \quad (35)$$

$$> 0, \quad \text{for } m > 1 \text{ and } p_{\text{success}} \in (0, 1). \quad (36)$$

\square

Corollary A.5 (Effective Sample Efficiency). *PRPO achieves an effective sample size of mG while maintaining the computational cost of m forward passes with G rollouts each. The improvement in reward signal density is:*

$$\frac{P_{\text{PRPO}}}{P_{\text{GRPO}}} = \frac{1 - (1 - p_{\text{success}})^{mG}}{1 - (1 - p_{\text{success}})^G}. \quad (37)$$

For small p_{success} (sparse reward setting), this ratio approaches m , indicating near-linear improvement.

A.5. Policy Gradient Analysis

Theorem A.6 (Unbiasedness of PRPO Gradient). *The PRPO policy gradient is an unbiased estimator of the true policy gradient:*

$$\mathbb{E} [\nabla_{\theta} L^{\text{PRPO}}(\theta)] = \nabla_{\theta} J(\theta), \quad (38)$$

where $J(\theta) = \mathbb{E}_{x, o \sim \pi_{\theta}} [R(o)]$ is the expected reward.

Proof. The PRPO objective is:

$$L^{\text{PRPO}}(\theta) = \mathbb{E}_x \left[\sum_{k=1}^m \sum_{i=1}^G \min \left(r_{k,i}(\theta) \hat{A}_{k,i}^{\text{PRPO}}, \text{clip}(r_{k,i}(\theta), 1 - \epsilon, 1 + \epsilon) \hat{A}_{k,i}^{\text{PRPO}} \right) \right]. \quad (39)$$

Taking the gradient and using the policy gradient theorem:

$$\nabla_{\theta} L^{\text{PRPO}}(\theta) = \mathbb{E}_x \left[\sum_{k=1}^m \sum_{i=1}^G \nabla_{\theta} \log \pi_{\theta}(o_{k,i} | q_k) \cdot \hat{A}_{k,i}^{\text{PRPO}} \right] \quad (40)$$

$$= \mathbb{E}_x \left[\sum_{k=1}^m \sum_{i=1}^G \nabla_{\theta} \log \pi_{\theta}(o_{k,i} | q_k) \cdot \left(\alpha \hat{A}_{k,i}^{(1)} + (1 - \alpha) \hat{A}_{k,i}^{(2)} \right) \right]. \quad (41)$$

Since both $\hat{A}_{k,i}^{(1)}$ and $\hat{A}_{k,i}^{(2)}$ are centered (zero-mean) advantage estimates, and the permutations preserve the semantic content of the input, the gradient is unbiased:

$$\mathbb{E} [\nabla_{\theta} L^{\text{PRPO}}(\theta)] = \nabla_{\theta} \mathbb{E}_{x, o \sim \pi_{\theta}} [R(o)] = \nabla_{\theta} J(\theta). \quad (42)$$

□

A.6. Convergence Analysis

Theorem A.7 (Convergence of PRPO). *Under standard assumptions (bounded rewards, Lipschitz continuous policy, bounded variance), PRPO converges to a stationary point of the expected reward objective. Specifically, for learning rate $\eta_t = O(1/\sqrt{t})$:*

$$\min_{t \leq T} \mathbb{E} [\|\nabla_{\theta} J(\theta_t)\|^2] = O\left(\frac{1}{\sqrt{T}}\right). \quad (43)$$

Proof. The proof follows the standard analysis of stochastic gradient descent with variance reduction.

Step 1: Smoothness assumption. Assume $J(\theta)$ is L -smooth:

$$J(\theta') \leq J(\theta) + \nabla J(\theta)^{\top} (\theta' - \theta) + \frac{L}{2} \|\theta' - \theta\|^2. \quad (44)$$

Step 2: Descent lemma. For the update $\theta_{t+1} = \theta_t + \eta_t g_t$ where $g_t = \nabla_{\theta} L^{\text{PRPO}}(\theta_t)$:

$$J(\theta_{t+1}) \leq J(\theta_t) + \eta_t \nabla J(\theta_t)^{\top} \mathbb{E}[g_t] + \frac{L\eta_t^2}{2} \mathbb{E}[\|g_t\|^2] \quad (45)$$

$$= J(\theta_t) + \eta_t \|\nabla J(\theta_t)\|^2 + \frac{L\eta_t^2}{2} (\|\nabla J(\theta_t)\|^2 + \text{Var}[g_t]). \quad (46)$$

Step 3: Variance bound. By Theorem A.3, $\text{Var}[g_t] \leq \sigma_{\text{PRPO}}^2 \leq \sigma_{\text{GRPO}}^2$.

Step 4: Telescoping sum. Summing over $t = 1, \dots, T$ and rearranging:

$$\sum_{t=1}^T \eta_t \|\nabla J(\theta_t)\|^2 \leq J(\theta_1) - J(\theta_{T+1}) + \frac{L}{2} \sum_{t=1}^T \eta_t^2 (\|\nabla J(\theta_t)\|^2 + \sigma_{\text{PRPO}}^2). \quad (47)$$

Step 5: Final bound. For $\eta_t = \eta/\sqrt{T}$ with appropriate η :

$$\min_{t \leq T} \|\nabla J(\theta_t)\|^2 \leq \frac{J(\theta_1) - J^* + L\eta^2 \sigma_{\text{PRPO}}^2}{\eta\sqrt{T}} = O\left(\frac{1}{\sqrt{T}}\right). \quad (48)$$

□

A.7. Comparison with GRPO

Proposition A.8 (PRPO Dominates GRPO in Sparse Reward Settings). *In the sparse reward setting where $p_{\text{success}} \ll 1$, PRPO achieves faster convergence than GRPO. Specifically, let T_{GRPO} and T_{PRPO} denote the number of iterations required to achieve ϵ -optimality. Then:*

$$\frac{T_{\text{GRPO}}}{T_{\text{PRPO}}} \geq \frac{\sigma_{\text{GRPO}}^2}{\sigma_{\text{PRPO}}^2} \cdot \frac{P_{\text{PRPO}}}{P_{\text{GRPO}}} \approx m, \quad (49)$$

for small p_{success} and optimal choice of α .

Proof. From Theorem A.7, the convergence rate depends on σ^2/\sqrt{T} . To achieve the same ϵ -optimality:

$$\frac{\sigma_{\text{GRPO}}^2}{\sqrt{T_{\text{GRPO}}}} = \frac{\sigma_{\text{PRPO}}^2}{\sqrt{T_{\text{PRPO}}}}. \quad (50)$$

Additionally, the effective learning signal per iteration is proportional to the probability of receiving positive rewards. Combining these factors:

$$\frac{T_{\text{GRPO}}}{T_{\text{PRPO}}} = \left(\frac{\sigma_{\text{GRPO}}^2}{\sigma_{\text{PRPO}}^2} \right)^2 \cdot \frac{P_{\text{PRPO}}}{P_{\text{GRPO}}}. \quad (51)$$

For sparse rewards ($p_{\text{success}} \ll 1$), by Corollary A.5, $P_{\text{PRPO}}/P_{\text{GRPO}} \approx m$. Combined with the variance reduction from Theorem A.3, PRPO achieves approximately m -fold speedup. \square

B. PRPO Fine-tuning Setting

The hyperparameters and training configurations of PRPO for our model is provided in Table 6.

Table 6. Key hyperparameters and environment settings for PRPO fine-tuning on **our model**.

Parameter	Value
Base model	Qwen3-8B-Base
Training batch size	128
PPO mini-batch size	32
Micro-batch per GPU	4
Max prompt length	5120
Max response length	1024
Learning rate	1×10^{-6}
KL loss coefficient β	0.001
number of permutations m	4
intra-permutation advantages coefficient α	0.1
inter-permutation advantages coefficient γ	0.9
Entropy coefficient	0
Rollout parallel size	2
Number of rollouts per sample G	5
GPU memory utilization	0.6
Number of GPUs per node	8
Number of nodes	1
Total training epochs	30
CUDA version	12.6

C. Data

C.1. Data distribution

To enable LLMs to acquire robust tabular reasoning capabilities through PRPO, the collection of diverse and sufficiently large tabular datasets is essential. We collected 139 public datasets from OpenML, covering a wide range of application domains. To comprehensively evaluate the capability of our method, datasets from different domains are divided into two groups: one subset is used for fully trained experiments to assess supervised performance, while the other is used for zero-shot and few-shot experiments to evaluate general reasoning ability across unseen domains. The overall domain distribution of these datasets is illustrated in Figure 6.

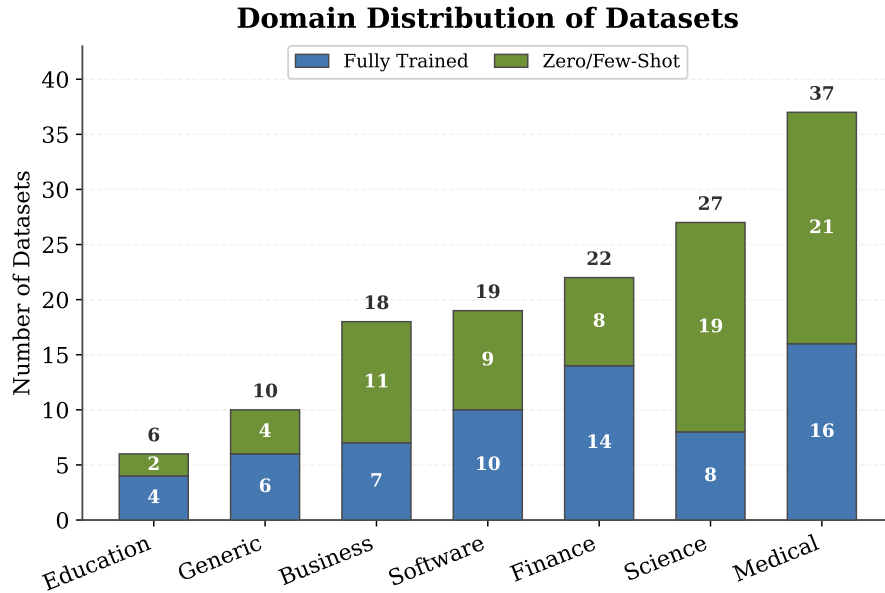


Figure 6. Domain distribution of fully trained and zero-/few-shot datasets.

C.2. Detailed Information of Datasets

To provide a clear overview of the datasets used in our experiments, we summarize the detailed information of the 139 OpenML datasets in this section. Each dataset includes its abbreviation, full name, experimental setting, domain classification, and OpenML reference. These datasets cover a wide variety of tasks and domains, forming the foundation for our fully trained, zero-shot, and few-shot experiments.

In the experimental result tables (Table 1, Table 2, Table 3, Table 4), we use abbreviated dataset names for brevity. Table 7 presents the full names of all datasets used in the experiments. Table 8 summarizes the experimental settings and corresponding domain classifications for each dataset, while Table 9 provides the OpenML IDs and URLs for reference and reproducibility.

Table 7. Abbreviations and full names of the OpenML datasets used in our experiments.

Dataset Abbreviation	Full dataset name
1000	1000_Cameras_Dataset
AAPL	AAPL_stock_price_2021_2022
AVIDa	AVIDa_SARS_CoV_2

Continued on next page

(continued)

<i>Dataset Abbreviation</i>	<i>Full dataset name</i>
Amazo	Amazon_employee_access_seed_0_nrows_2000_nclasses_10_ncols_100_stratify_True
Bank	Bank_Customer_Churn
Bosto	Boston_house_price_data
CPMP	CPMP_2015_runtime_regression
Carpe	CarpenterFdaData
Click	Click_prediction_small_seed_0_nrows_2000_nclasses_10_ncols_100_stratify_True
Emplo	Employee
Fraud	Fraud_Detection_Updated
Goodr	Goodreads_Computer_Books
HMEQ	HMEQ_Data
Lisbo	Lisbon_House_Prices
Loan	Loan_Predication
MIP	MIP_2016_regression
Mammo	Mammographic_Mass_Data_Set
Marke	Marketing_Campaign
NATIC	NATICUSdroid
NHANE	NHANES_age
PostP	PostPartum_Depression
SPECT	SPECTF
Skin	Skin_Cancer_PAD_UFES_20
Speed	SpeedDating
Tour	Tour_and_Travels_Customer_Churn_Prediction
Tunin	TuningSVMs
UCI	UCI_churn
WMO	WMO_Hurricane_Survival_Dataset
ada	ada_prior
adult	adult_seed_0_nrows_2000_nclasses_10_ncols_100_stratify_True
airli	airlines_seed_0_nrows_2000_nclasses_10_ncols_100_stratify_True
ames	ames_housing
analc	analcata_data_apnea1
annea	anneal
arrhy	arrhythmia
arsen	arsenic_female_bladder
art	art_daily_nojump4
aucti	auction_verification
autoM	autoMpg
blast	blastchar
blood	blood_transfusion_service_center
brazi	braziltourism
breas	breast_cancer
breas	breast_w
bwin	bwin_amlb
calif	california_seed_0_nrows_2000_nclasses_10_ncols_100_stratify_True
cars	cars
chole	cholesterol
chole	cholesterol
churn	churn
cleve	cleve
coffe	coffee_distribution_across_94_counties
coil2	coil2000_insurance_policies
colic	colic
colre	colrec
commu	communities_and_crime_binary
compa	compas_two_years

Continued on next page

(continued)

<i>Dataset Abbreviation</i>	<i>Full dataset name</i>
concr	concrete_compressive_strength
confe	conference_attendance
datas	dataset_credit_g
datat	datatrieve
depre	depression_2020
dgf	dgf_test
diabe	diabetes
diffe	differentiated_thyroid_cancer_recurrence
dis	dis
discl	disclosure_x_noise
doa	doa_bwin
e1684	e1684
emplo	employee_salaries
eye	eye_movements
flags	flags
haber	haberman
hayes	hayes_roth
healt	healthcare_insurance_expenses
hepat	hepatitis
house	house_prices
hypot	hypothyroid
ibm	ibm_employee_attrition
imdb	imdb_genre_prediction
ipums	ipums_la_98_small
iris	iris
irish	irish
jungl	jungle_chess_2pcs_endgame_elephant_elephant
kc1	kc1
kc2	kc2
kc3	kc3
kdd	kdd_el_nino_small
kick	kick_seed_0_nrows_2000_nclasses_10_ncols_100_stratify_True
lowbw	lowbwt
lungc	lungcancer_GSE31210
mauna	mauna_loa_atmospheric_co2
mc1	mc1
mc2	mc2
meta	meta
munic	munich_rent_index_1999
mw1	mw1
newto	newton_hema
newto	newton_hema
no2	no2
nwtco	nwtco
page	page_blocks
pakis	pakistan_hunger_data
pc1	pc1
pc2	pc2
pc3	pc3
pc4	pc4
phary	pharynx
place	places
plasm	plasma_retinol
plasm	plasma_retinol

Continued on next page

(continued)

<i>Dataset Abbreviation</i>	<i>Full dataset name</i>
pm10	pm10
pm10	pm10
polis	polish_companies_bankruptcy
polle	pollen
prnn	prnn_crabs
profb	profb
quake	quake
regim	regime_alimentaire
road	road_safety_seed_0_nrows_2000_nclasses_10_ncols_100_stratify_True
segme	segment
seism	seismic_bumps
seoul	seoul_bike_sharing_demand_cat
solar	solar_flare
spamb	spambase
spect	spectrometer
std	std
taiwa	taiwanese_bankruptcy_prediction
telco	telco_customer_churn
tempe	temperature_emissions_environmental_trends_2000_2024
tic	tic_tac_toe
triaz	triazines
tumor	tumor
vehic	vehicle
vowel	vowel
weath	weather_ankara
wilt	wilt
wisco	wisconsin
yacht	yacht_hydrodynamics

Table 8. Experimental settings and domain categories of the datasets.

Dataset abbreviation	experiment_setting	domain
1000	regression_fully_trained	software
AAPL	regression_fully_trained	finance
AVIDa	classification_fully_trained	medical
Amazo	classification_fully_trained	finance
Bank	classification_zero_few_shot	finance
Bosto	regression_zero_few_shot	business
CPMP	regression_zero_few_shot	software
Carpe	regression_fully_trained	medical
Click	classification_fully_trained	finance
Emplo	classification_zero_few_shot	business
Fraud	classification_fully_trained	finance
Goodr	regression_fully_trained	education
HMEQ	classification_zero_few_shot	finance
Lisbo	regression_zero_few_shot	business
Loan	classification_fully_trained	finance
MIP	regression_fully_trained	finance
Mammo	classification_fully_trained	medical
Marke	classification_fully_trained	business

(continued)

Dataset abbreviation	experiment_setting	domain
NATIC	classification_zero_few_shot	software
NHANE	regression_zero_few_shot	medical
PostP	classification_zero_few_shot	medical
SPECT	classification_zero_few_shot	medical
Skin	classification_zero_few_shot	medical
Speed	classification_fully_trained	business
Tour	classification_zero_few_shot	finance
Tunin	classification_zero_few_shot	education
UCI	classification_zero_few_shot	finance
WMO	classification_fully_trained	generic
ada	classification_fully_trained	generic
adult	classification_zero_few_shot	finance
airli	classification_zero_few_shot	business
ames	regression_zero_few_shot	business
analc	classification_zero_few_shot	medical
annea	classification_zero_few_shot	science
arrhy	classification_zero_few_shot	medical
arsen	classification_fully_trained	medical
art	classification_fully_trained	science
aucti	regression_zero_few_shot	business
autoM	classification_zero_few_shot	science
blast	classification_zero_few_shot	business
blood	classification_fully_trained	medical
brazi	classification_zero_few_shot	business
breas	classification_fully_trained	medical
breas	classification_fully_trained	medical
bwin	classification_fully_trained	finance
calif	classification_zero_few_shot	generic
cars	regression_zero_few_shot	business
chole	classification_zero_few_shot	medical
chole	regression_fully_trained	medical
churn	classification_zero_few_shot	finance
cleve	classification_zero_few_shot	medical
coffe	regression_fully_trained	business
coil2	classification_fully_trained	finance
colic	classification_zero_few_shot	medical
colre	regression_zero_few_shot	software
commu	classification_zero_few_shot	science
compa	classification_zero_few_shot	generic
concr	regression_zero_few_shot	software
confe	classification_fully_trained	business
datas	classification_fully_trained	finance
datat	classification_fully_trained	education
depre	classification_fully_trained	medical
dgf	classification_zero_few_shot	generic
diabe	classification_zero_few_shot	medical
diffe	classification_zero_few_shot	medical
dis	classification_fully_trained	medical
discl	regression_fully_trained	generic
doa	classification_fully_trained	finance

Continued on next page

(continued)

Dataset abbreviation	experiment_setting	domain
e1684	regression_fully_trained	medical
emplo	regression_zero_few_shot	business
eye	classification_zero_few_shot	science
flags	classification_zero_few_shot	generic
haber	classification_fully_trained	medical
hayes	classification_zero_few_shot	education
healt	regression_zero_few_shot	medical
hepat	classification_zero_few_shot	medical
house	regression_zero_few_shot	business
hypot	classification_zero_few_shot	medical
ibm	classification_zero_few_shot	finance
imdb	classification_fully_trained	education
ipums	classification_fully_trained	generic
iris	classification_fully_trained	science
irish	classification_fully_trained	science
jungl	classification_zero_few_shot	software
kc1	classification_fully_trained	software
kc2	classification_zero_few_shot	software
kc3	classification_fully_trained	software
kdd	classification_zero_few_shot	science
kick	classification_fully_trained	finance
lowbw	regression_zero_few_shot	medical
lungc	classification_zero_few_shot	medical
mauna	regression_zero_few_shot	science
mc1	classification_fully_trained	software
mc2	classification_fully_trained	software
meta	classification_fully_trained	education
munic	regression_fully_trained	finance
mw1	classification_fully_trained	software
newto	classification_zero_few_shot	medical
newto	regression_zero_few_shot	medical
no2	classification_zero_few_shot	science
nwtco	regression_fully_trained	medical
page	classification_zero_few_shot	software
pakis	regression_fully_trained	business
pc1	classification_fully_trained	software
pc2	classification_fully_trained	software
pc3	classification_fully_trained	software
pc4	classification_fully_trained	software
phary	classification_zero_few_shot	medical
place	regression_zero_few_shot	science
plasm	classification_fully_trained	medical
plasm	regression_fully_trained	medical
pm10	classification_zero_few_shot	science
pm10	regression_zero_few_shot	science
polis	classification_fully_trained	finance
polle	classification_fully_trained	science
prnn	classification_zero_few_shot	science
profb	classification_fully_trained	business
quake	classification_fully_trained	science

Continued on next page

(continued)

Dataset abbreviation	experiment_setting	domain
regim	classification_fully_trained	business
road	classification_zero_few_shot	science
segme	classification_zero_few_shot	software
seism	classification_fully_trained	generic
seoul	regression_zero_few_shot	science
solar	classification_fully_trained	science
spamb	classification_zero_few_shot	software
spect	classification_zero_few_shot	science
std	regression_zero_few_shot	medical
taiwa	classification_fully_trained	finance
telco	classification_zero_few_shot	finance
tempe	regression_fully_trained	science
tic	classification_fully_trained	generic
triaz	classification_zero_few_shot	science
tumor	regression_fully_trained	medical
vehic	classification_zero_few_shot	science
vowel	classification_zero_few_shot	science
weath	regression_zero_few_shot	science
wilt	classification_fully_trained	science
wisco	classification_zero_few_shot	medical
yacht	regression_zero_few_shot	science

Table 9. OpenML IDs and URLs of the datasets for reference.

Dataset abbreviation	openml_ID	openml_URL
1000	43714	https://www.openml.org/d/43714
AAPL	43878	https://www.openml.org/d/43878
AVIDa	46800	https://www.openml.org/d/46800
Amazo	44708	https://www.openml.org/d/44708
Bank	46911	https://www.openml.org/d/46911
Bosto	43465	https://www.openml.org/d/43465
CPMP	41928	https://www.openml.org/d/41928
Carpe	46159	https://www.openml.org/d/46159
Click	44763	https://www.openml.org/d/44763
Emplo	46925	https://www.openml.org/d/46925
Fraud	46359	https://www.openml.org/d/46359
Goodr	43785	https://www.openml.org/d/43785
HMEQ	46431	https://www.openml.org/d/46431
Lisbo	43660	https://www.openml.org/d/43660
Loan	43595	https://www.openml.org/d/43595
MIP	43070	https://www.openml.org/d/43070
Mammo	45557	https://www.openml.org/d/45557
Marke	46940	https://www.openml.org/d/46940
NATIC	46969	https://www.openml.org/d/46969
NHANE	46946	https://www.openml.org/d/46946
PostP	46758	https://www.openml.org/d/46758
SPECT	337	https://www.openml.org/d/337
Skin	46630	https://www.openml.org/d/46630
Speed	40536	https://www.openml.org/d/40536
Tour	45545	https://www.openml.org/d/45545

Continued on next page

(continued)

Dataset abbreviation	openml_ID	openml_URL
Tunin	41976	https://www.openml.org/d/41976
UCI	44232	https://www.openml.org/d/44232
WMO	43607	https://www.openml.org/d/43607
ada	1037	https://www.openml.org/d/1037
adult	44723	https://www.openml.org/d/44723
airli	44528	https://www.openml.org/d/44528
ames	43926	https://www.openml.org/d/43926
analc	767	https://www.openml.org/d/767
annea	989	https://www.openml.org/d/989
arrhy	1017	https://www.openml.org/d/1017
arsen	949	https://www.openml.org/d/949
art	43051	https://www.openml.org/d/43051
aucti	44958	https://www.openml.org/d/44958
autoM	831	https://www.openml.org/d/831
blast	46280	https://www.openml.org/d/46280
blood	46913	https://www.openml.org/d/46913
brazi	957	https://www.openml.org/d/957
breas	13	https://www.openml.org/d/13
breas	15	https://www.openml.org/d/15
bwin	45717	https://www.openml.org/d/45717
calif	44362	https://www.openml.org/d/44362
cars	46914	https://www.openml.org/d/46914
chole	798	https://www.openml.org/d/798
chole	204	https://www.openml.org/d/204
churn	40701	https://www.openml.org/d/40701
cleve	40710	https://www.openml.org/d/40710
coffe	46748	https://www.openml.org/d/46748
coil2	46916	https://www.openml.org/d/46916
colic	25	https://www.openml.org/d/25
colre	46145	https://www.openml.org/d/46145
commu	43891	https://www.openml.org/d/43891
compa	42192	https://www.openml.org/d/42192
concr	44959	https://www.openml.org/d/44959
confe	41538	https://www.openml.org/d/41538
datas	46532	https://www.openml.org/d/46532
datat	1075	https://www.openml.org/d/1075
depre	46876	https://www.openml.org/d/46876
dgf	42882	https://www.openml.org/d/42882
diabe	37	https://www.openml.org/d/37
diffe	46605	https://www.openml.org/d/46605
dis	40713	https://www.openml.org/d/40713
discl	704	https://www.openml.org/d/704
doa	45711	https://www.openml.org/d/45711
e1684	46157	https://www.openml.org/d/46157
emplo	42125	https://www.openml.org/d/42125
eye	43946	https://www.openml.org/d/43946
flags	1012	https://www.openml.org/d/1012
haber	43	https://www.openml.org/d/43
hayes	974	https://www.openml.org/d/974
healt	46931	https://www.openml.org/d/46931

Continued on next page

(continued)

Dataset abbreviation	openml_ID	openml_URL
hepat	55	https://www.openml.org/d/55
house	42165	https://www.openml.org/d/42165
hypot	1000	https://www.openml.org/d/1000
ibm	43893	https://www.openml.org/d/43893
imdb	46667	https://www.openml.org/d/46667
ipums	1002	https://www.openml.org/d/1002
iris	969	https://www.openml.org/d/969
irish	451	https://www.openml.org/d/451
jung1	40999	https://www.openml.org/d/40999
kc1	1067	https://www.openml.org/d/1067
kc2	1063	https://www.openml.org/d/1063
kc3	1065	https://www.openml.org/d/1065
kdd	839	https://www.openml.org/d/839
kick	44758	https://www.openml.org/d/44758
lowbw	203	https://www.openml.org/d/203
lungc	1412	https://www.openml.org/d/1412
mauna	41187	https://www.openml.org/d/41187
mc1	1056	https://www.openml.org/d/1056
mc2	1054	https://www.openml.org/d/1054
meta	757	https://www.openml.org/d/757
munic	46772	https://www.openml.org/d/46772
mw1	1071	https://www.openml.org/d/1071
newto	784	https://www.openml.org/d/784
newto	492	https://www.openml.org/d/492
no2	886	https://www.openml.org/d/886
nwtco	46165	https://www.openml.org/d/46165
page	1021	https://www.openml.org/d/1021
pakis	46732	https://www.openml.org/d/46732
pc1	1068	https://www.openml.org/d/1068
pc2	1069	https://www.openml.org/d/1069
pc3	1050	https://www.openml.org/d/1050
pc4	1049	https://www.openml.org/d/1049
phary	738	https://www.openml.org/d/738
place	509	https://www.openml.org/d/509
plasm	915	https://www.openml.org/d/915
plasm	511	https://www.openml.org/d/511
pm10	750	https://www.openml.org/d/750
pm10	522	https://www.openml.org/d/522
polis	46950	https://www.openml.org/d/46950
polle	871	https://www.openml.org/d/871
prnn	446	https://www.openml.org/d/446
profb	470	https://www.openml.org/d/470
quake	772	https://www.openml.org/d/772
regim	42172	https://www.openml.org/d/42172
road	44453	https://www.openml.org/d/44453
segme	958	https://www.openml.org/d/958
seism	45562	https://www.openml.org/d/45562
seoul	46328	https://www.openml.org/d/46328
solar	40702	https://www.openml.org/d/40702
spamb	44	https://www.openml.org/d/44

Continued on next page

(continued)

Dataset abbreviation	openml_ID	openml_URL
spect	954	https://www.openml.org/d/954
std	46156	https://www.openml.org/d/46156
taiwa	46962	https://www.openml.org/d/46962
telco	42178	https://www.openml.org/d/42178
tempe	46731	https://www.openml.org/d/46731
tic	50	https://www.openml.org/d/50
triaz	788	https://www.openml.org/d/788
tumor	46171	https://www.openml.org/d/46171
vehic	994	https://www.openml.org/d/994
vowel	1016	https://www.openml.org/d/1016
weath	42368	https://www.openml.org/d/42368
wilt	40983	https://www.openml.org/d/40983
wisco	753	https://www.openml.org/d/753
yacht	42370	https://www.openml.org/d/42370

C.3. Text template for our model

In this subsection, we introduce the detailed design of the serialization template. The template is designed to convert tabular data into structured textual inputs that can be effectively processed by the LLMs. Each feature–value pair in the table is expressed as a short, human-readable clause (e.g., “The [feature] is [value].”) and concatenated in a fixed column order to form a complete instance representation. The prompt consists of two components: (1) a system instruction that defines the model’s role as a tabular prediction expert and guides its internal reasoning, and (2) a user message that includes the serialized feature descriptions and a task-specific prediction question.

We further wrap the model’s reasoning and final prediction with `< think >` and `< answer >` tags, respectively, to clearly separate the reasoning process from the final output. This design enables our model to perform effective reasoning over tabular data and provides verifiable reward signals for reinforcement learning. It serves as the data foundation of PRPO, facilitating our model’s learning of tabular reasoning patterns. The text templates for classification and regression tasks are shown below.

Example of the text template used for a classification task in our model

System

Role: You are an expert in tabular prediction. When addressing tabular prediction tasks, you first conduct analysis and reasoning in your mind before presenting the prediction results to the user.

User

Input: The Married is Yes. The Education is Graduate. The LoanAmount is 44.0. The CoapplicantIncome is 0.0. The Gender is Male. The ApplicantIncome is 5649. The Property_Area is Urban. The Dependents is 1. The Self_Employed is No. The Loan_Amount_Term is 360.0. The Credit_History is 1.0.

Task: Will the applicant’s loan be approved? yes or no?

Output Format: Show your analysis and reasoning in `<think>` `</think>` tags. And return the final answer in `<answer>` `</answer>` tags.

Example of the text template used for a regression task in our model

System

Role: You are an expert in tabular prediction. When addressing tabular prediction tasks, you first conduct analysis and reasoning in your mind before presenting the prediction results to the user.

User

Input: The City is Hyderabad. The Year is 2022. The Population_Under_Poverty is 29.1. The Malnutrition_Rate is 15.1. The Food_Insecurity is 21.2. The Access_to_Clean_Water is 83.5. The Food_Production_Index is 96.5.

Task: What is the percentage of children who are underweight in that city?

Output Format: Show your analysis and reasoning in `<think>` `</think>` tags. And return the final answer in `<answer>` `</answer>` tags.

C.4. Text template for Qwen and DeepSeek-R1 series models

In the experiments presented in Table 2 and Table 4, the Qwen and DeepSeek-R1 series models are evaluated under the zero-shot setting. The text templates for classification and regression tasks are shown below.

Example of the text template used for the zero-shot evaluation of Qwen and DeepSeek-R1 series models on classification tasks

System

Role: You are a helpful assistant.

User

Input: The Married is Yes. The Education is Graduate. The LoanAmount is 44.0. The CoapplicantIncome is 0.0. The Gender is Male. The ApplicantIncome is 5649. The Property_Area is Urban. The Dependents is 1. The Self_Employed is No. The Loan_Amount_Term is 360.0. The Credit_History is 1.0.

Task: Will the applicant’s loan be approved? yes or no?

Output Format: Return the final answer in `<answer>` `</answer>` tags.

Example of the text template used for the zero-shot evaluation of Qwen and DeepSeek-R1 series models on regression tasks

System

Role: You are a helpful assistant.

User

Input: The City is Hyderabad. The Year is 2022. The Population_Under_Poverty is 29.1. The Malnutrition_Rate is 15.1. The Food_Insecurity is 21.2. The Access_to_Clean_Water is 83.5. The Food_Production_Index is 96.5.

Task: What is the percentage of children who are underweight in that city?

Output Format: Return the final answer in `<answer>` `</answer>` tags.

D. Reasoning Example

In this subsection, we illustrate the reasoning process of our model. An example of our model’s reasoning process for a classification task is shown below.

An example of our model’s reasoning process on a classification task

System

Role: You are an expert in tabular prediction. When addressing tabular prediction tasks, you first conduct analysis and reasoning in your mind before presenting the prediction results to the user.

User

Input: The state is 2.0. The account_length is 110.0. The area_code is 408.0. The phone_number is 2398.0. The international_plan is 0.0. The voice_mail_plan is 0.0. The number_vmail_messages is 0.0. The total_day_minutes is 55.3. The total_day_calls is 102.0. The total_day_charge is 9.4. The total_eve_minutes is 164.7. The total_eve_calls is 124.0. The total_eve_charge is 14.0. The total_night_minutes is 200.7. The total_night_calls is 108.0. The total_night_charge is 9.03. The total_intl_minutes is 10.2. The total_intl_calls is 5.0. The total_intl_charge is 2.75. The number_customer_service_calls is 1.0.

Task: Will this customer churn (leave the telecom service)? yes or no?

Output Format: Show your analysis and reasoning in `<think>` `</think>` tags. And return the final answer in `<answer>` `</answer>` tags.

Assistant

Reasoning: `<think>`
 To determine whether this customer will churn, I examine the profile from several complementary perspectives: service usage, billing pressure, customer support interactions, and long-term retention signals. Churn is usually associated with repeated service issues, unusual cost burden, or very short account age. In this example, most of the evidence points in the opposite direction.

Step-by-step assessment:

1. **Account longevity.** The account length is 110 months, which is a strong indicator of customer stability and lower churn risk.
2. **Customer support burden.** The number of customer service calls is only 1, so a major dissatisfaction signal is absent.
3. **Daytime usage profile.** The customer has regular daytime usage, and the associated charge remains modest.
4. **Evening and night behavior.** The evening and night usage values are also within a normal range, without signs of unusual cost pressure or disengagement.
5. **International activity.** The customer does not have an international plan, but the international usage is not excessive, so the related charge is unlikely to create serious billing frustration.
6. **Voice mail and feature adoption.** The customer does not use a voice mail plan, which appears to reflect preference rather than dissatisfaction.
7. **Overall cost structure.** Looking across day, evening, night, and international charges together, the total spending pattern appears moderate rather than extreme. Customers facing unusually high bills are more likely to leave, but that pattern is not visible here.
8. **Absence of classic red flags.** Common churn indicators include repeated support calls, abnormal charges, very short tenure, or unstable usage patterns. This customer does not exhibit any of those major warning signs.

Synthesis: The strongest evidence comes from the long account history and the very low number of customer service calls. The usage profile is steady, the charges are not alarming, and there is no obvious mismatch between services used and services available. Overall, this customer appears more likely to stay than to leave.

Conclusion: Based on the customer’s usage patterns, cost structure, service interaction history, and long tenure, the most likely prediction is that this customer will *not* churn. `</think>`

Final Answer

`<answer>no</answer>`

An example of our model’s reasoning process for a regression task is shown below.

An example of our model’s reasoning process on a regression task

System

Role: You are an expert in tabular prediction. When addressing tabular prediction tasks, you first conduct analysis and reasoning in your mind before presenting the prediction results to the user.

User

Input: The book_Title is Schaum’s Outline of Computer Architecture. The Author_Name is Nick Carter. The ratings_count is 24.0. The Publish_year is 2001. The Edition is 2. The Pages_no is 306. The Book_language is English. The Reviews is 2.

Task: Based on a computer science book’s title, author, ratings count, publication year, edition number, page count, language, and number of reviews, what is its average rating on Goodreads?

Output Format: Show your analysis and reasoning in `<think>` `</think>` tags. And return the final answer in `<answer>` `</answer>` tags.

Assistant

Reasoning: `<think>`
 To estimate the average Goodreads rating for this book, I consider the title, author information, edition number, publication year, length, and amount of reader feedback. In a regression setting like this, the goal is to infer a plausible value on the rating scale by combining multiple weak signals.

Step-by-step assessment:

1. **Title semantics.** The title “Schaum’s Outline of Computer Architecture” strongly suggests that the book is an educational outline or study guide.
2. **Domain and audience.** Computer architecture is a technical subject, and readers often reward accuracy, structure, and practical usefulness.
3. **Author signal.** The named author provides some credibility, although by itself the author name is not enough to imply an exceptionally high score. It is more reasonable to view this as a mild positive signal than as decisive evidence for a very high rating.
4. **Edition number.** The book is in its second edition, which is usually a favorable sign because it suggests the material was useful enough to justify revision.
5. **Publication year.** The book was published in 2001. For a foundational technical topic, this is not so old that the content would automatically be viewed as obsolete.
6. **Length and scope.** The page count of 306 suggests moderate coverage: substantial enough to be useful, but not overwhelmingly long.
7. **Ratings count and reviews.** The book has only 24 ratings and 2 reviews. Low feedback volume means the average score may be noisy, but it still suggests some positive reader engagement.
8. **Expected score range.** Combining the educational nature of the book, the second edition, moderate length, and limited but nonzero engagement, the most plausible estimate is a rating that is clearly positive but not outstandingly high. In other words, the metadata supports a score above average, but not enough evidence is present to push the estimate confidently into an exceptional range.

Synthesis: I would not expect the book to fall near the low end of the scale, because the metadata suggests a legitimate and useful technical resource. The second edition, moderate page count, and technical focus all support a favorable evaluation. At the same time, the small number of ratings and the specialized nature of the subject make an extremely high score less certain. This points to a value in the high 3s rather than the mid 4s.

Conclusion: Considering the title, domain, edition information, moderate page count, and limited but positive-seeming feedback footprint, a reasonable estimate for the average Goodreads rating is about 3.9. `</think>`

Final Answer

Given these considerations, the average rating can be estimated to be around `<answer>3.9</answer>`.

E. Hyperparameter tuning of XGBoost and TabPFN v2

In this section, we introduce the hyperparameter tuning and experimental setup of the two baseline models used in our experiments, XGBoost and TabPFN.

E.1. XGBoost

We adopted the XGBoost classifier for both binary and multi-class classification tasks. Hyperparameters were optimized using the Optuna framework with a random search strategy (RandomSampler), minimizing the log-loss on the training set. Each dataset was split into 80% training and 20% testing subsets using a stratified split, with label encoding applied to categorical targets. For categorical features, a one-hot encoder was used, while numerical or string-valued columns were coerced to numeric values. Each optimization trial trained a model using early stopping and evaluated the log-loss to guide parameter selection. We used the same hyperparameter search space as (Shwartz-Ziv & Armon, 2021), which is provided in Table 10.

Table 10. Hyperparameter search space for XGBoost.

baseline	name	type	log	range
XGBoost	learning_rate	float	$[e^{-7}, 1]$	yes
	max_depth	int	$[1, 10]$	–
	subsample	float	$[0.2, 1]$	–
	colsample_bytree	float	$[0.2, 1]$	–
	colsample_bylevel	float	$[0.2, 1]$	–
	min_child_weight	float	$[e^{-16}, e^5]$	yes
	alpha	float	$[e^{-16}, e^2]$	yes
	lambda	float	$[e^{-16}, e^2]$	yes
	gamma	float	$[e^{-16}, e^2]$	yes
	n_estimators	int	$[100, 4000]$	–

E.2. TabPFN

For TabPFN, we employed the official *TabPFN Extensions* implementation and extended it to handle heterogeneous OpenML datasets containing missing or non-numeric features. Missing values were imputed using the most frequent strategy. Each dataset was evaluated under 10 independent runs with different random seeds $\{4, 8, 16, 32, 42, 64, 128, 256, 512, 1024\}$, using an 80/20 stratified train–test split per run. The TabPFN model used its default architecture and priors without additional hyperparameter tuning. We report the averaged Accuracy across runs.

F. More Results

Full Quantitative Results. Complete results of our experiments are detailed in Table 11, Table 12, Table 13 and Table 14.

Visual Analysis of Learning Dynamics. As shown in Figure 7a, the results reveal contrasting scaling dynamics: while baselines rely on increasing labeled data for monotonic improvement, our method establishes a superior zero-shot foundation that already exceeds the 16-shot results of competitors. This performance gap confirms that PRPO effectively instills robust tabular reasoning priors, significantly mitigating the reliance on task-specific supervision.

Data Efficiency. As illustrated in Figure 7b, under the zero-shot/few-shot setting, we quantify data efficiency by estimating the number of labeled samples each baseline requires to match our zero-shot performance via linear interpolation from their 4/8/16/32-shot results. On 53 classification datasets (a), reaching our zero-shot accuracy (70.2%) requires TabLLM 21 samples, XGBoost 26 samples, and TabPFN 34 samples per dataset for few-shot training. On 21 regression datasets (b), matching our zero-shot NMAE (0.1614) requires XGBoost 41 samples, while TabPFN needs only 7 samples. This analysis reveals that PRPO training effectively provides data efficiency equivalent to 21–41 labeled samples per dataset, demonstrating significant practical value for data-scarce scenarios.

Reinforcing Numerical Reasoning in LLMs for Tabular Prediction via Structural Priors

Table 11. Accuracy (\uparrow) comparison across models on classification datasets under the fully trained setting. Darker green cells indicate higher accuracy. All LLM-based methods except ours are evaluated under the zero-shot setting.

Dataset	Qwen2.5-7B	Qwen2.5-32B	Qwen3-8B	Qwen3-32B	Qwen3-235B	DS-R1	DS-0528	XGBoost	TabPFN	Ours
ada	0.7330	0.7943	0.7856	0.8118	0.7615	0.8249	0.8009	0.8313	0.8553	0.7834
Amazo	0.0600	0.0600	0.0850	0.3650	0.2400	0.9200	0.0700	0.9425	0.9425	0.9400
arsen	0.8750	0.8571	0.8036	0.6071	0.4107	0.0714	0.7500	0.8571	0.8723	0.8571
art	0.9678	0.9678	0.9678	0.9678	0.9356	0.8663	0.9604	0.9678	0.9678	0.9678
AVIDa	0.8021	0.8021	0.8021	0.8021	0.7995	0.6791	0.8021	0.8019	0.8019	0.8021
blood	0.4000	0.6133	0.4400	0.6800	0.7600	0.6667	0.4400	0.7600	0.7533	0.7600
breas	0.5172	0.5517	0.5862	0.6552	0.5172	0.6207	0.5517	0.7069	0.7500	0.7586
breas	0.9143	0.9143	0.8714	0.9857	0.9714	0.9571	0.8143	0.9429	0.9614	0.9571
bwin	0.5283	0.5849	0.3585	0.3962	0.3962	0.3774	0.4717	0.6698	0.6708	0.6604
Click	0.3750	0.8300	0.8050	0.4800	0.6050	0.5900	0.8000	0.8325	0.8305	0.8300
coil2	0.9400	0.8210	0.9379	0.9247	0.9217	0.8891	0.8566	0.9405	0.9405	0.9400
confe	0.4000	0.3600	0.6400	0.3600	0.5600	0.8000	0.4800	0.8800	0.8800	0.8800
datas	0.4200	0.4400	0.3200	0.3900	0.4900	0.5200	0.3200	0.7000	0.7045	0.7100
datat	0.8462	0.9231	0.8462	0.0769	0.5385	0.0769	0.7692	0.9231	0.9115	0.9231
depre	0.8322	0.7762	0.3007	0.2378	0.2797	0.2028	0.4336	0.8322	0.8322	0.8322
dis	0.9788	0.9815	0.9815	0.9762	0.9815	0.9762	0.9709	0.9841	0.9917	0.9841
doa	0.5849	0.4151	0.4906	0.5283	0.4528	0.3585	0.5660	0.6604	0.6321	0.6604
Fraud	0.8966	0.8942	0.7260	0.6635	0.4014	0.1971	0.3341	0.8990	0.9012	0.8990
haber	0.1935	0.6452	0.5484	0.5806	0.6452	0.5806	0.5484	0.7419	0.7484	0.7419
imdb	0.7875	0.8375	0.7875	0.8500	0.8625	0.8375	0.8000	0.7500	0.7556	0.8250
ipums	0.4766	0.6061	0.7210	0.6262	0.7784	0.7063	0.4806	0.8945	0.8951	0.8825
iris	1.0000	0.9333	1.0000	1.0000	1.0000	1.0000	1.0000	0.6667	1.0000	0.9333
irish	0.5600	0.9400	0.9000	1.0000	1.0000	1.0000	0.8400	1.0000	0.9910	1.0000
kc1	0.6445	0.5213	0.3886	0.7393	0.7346	0.6398	0.5592	0.8460	0.8507	0.8436
kc3	0.8261	0.9130	0.8913	0.7391	0.6739	0.5870	0.8696	0.9022	0.8804	0.9130
kick	0.7850	0.8650	0.6850	0.5550	0.1750	0.1250	0.4950	0.8775	0.8775	0.8750
Loan	0.7742	0.8226	0.7903	0.8065	0.7903	0.7903	0.7097	0.6911	0.7724	0.8226
Marke	0.6473	0.7366	0.7679	0.7946	0.7723	0.6429	0.7902	0.8504	0.8891	0.8750
mc1	0.6610	0.7360	0.7276	0.6589	0.6051	0.8353	0.8680	0.9926	0.9947	0.9916
mc2	0.8235	0.6471	0.5294	0.5294	0.5294	0.5882	0.5882	0.6667	0.6061	0.7059
meta	0.5472	0.5094	0.7925	0.6415	0.5472	0.0566	0.6415	0.8962	0.9208	0.9057
mw1	0.7073	0.6341	0.7073	0.6098	0.7561	0.5610	0.9268	0.9259	0.9284	0.9268
pc1	0.7297	0.4955	0.3694	0.5045	0.7387	0.3874	0.4144	0.9324	0.9423	0.9279
pc2	0.7943	0.9893	0.8372	0.7048	0.8354	0.6261	0.8927	0.9955	0.9954	0.9964
pc3	0.5669	0.7261	0.7452	0.4904	0.6561	0.5032	0.6624	0.8978	0.8994	0.8981
pc4	0.6096	0.6644	0.6438	0.5068	0.6644	0.5205	0.6233	0.8801	0.9199	0.8767
plasm	0.4375	0.2812	0.4688	0.4375	0.2500	0.5000	0.4375	0.5714	0.4762	0.5625
polis	0.7377	0.7614	0.3672	0.4450	0.4129	0.5482	0.1997	0.9306	0.9657	0.9306
polle	0.5091	0.4286	0.4935	0.4753	0.4831	0.3766	0.4857	0.4870	0.4688	0.5013
profb	0.0588	0.1029	0.0000	0.0294	0.2794	0.0735	0.0000	0.6741	0.6630	0.6618
quake	0.5000	0.5183	0.5596	0.5229	0.5229	0.5183	0.5321	0.5550	0.5532	0.5275
regim	1.0000	0.9524	1.0000	0.9048	0.9524	0.8571	1.0000	0.8049	0.9512	1.0000
seism	0.5869	0.6371	0.5637	0.4942	0.6062	0.3707	0.5830	0.9342	0.9323	0.9344
sf	0.8800	0.8150	0.8750	0.8250	0.7600	0.4600	0.8450	0.8775	0.8775	0.8800
solar	0.4019	0.2336	0.1776	0.2056	0.3458	0.2617	0.6822	0.8271	0.8037	0.8318
Speed	0.6301	0.4212	0.2780	0.6885	0.6420	0.6516	0.4654	0.8353	0.8648	0.8353
taiwa	0.9384	0.9677	0.0323	0.0367	0.0367	0.1349	0.0499	0.9677	0.9705	0.9677
tic	0.6146	0.9271	0.9896	0.9896	1.0000	1.0000	0.9792	0.7083	0.9880	1.0000
wilt	0.0579	0.0661	0.0909	0.1178	0.2831	0.1756	0.2955	0.9463	0.9889	0.9463
WMO	0.4851	0.4692	0.5050	0.5129	0.5109	0.5308	0.4771	0.5114	0.4955	0.5149
Mean	0.6409	0.6678	0.6196	0.5986	0.6175	0.5608	0.6187	0.8234	0.8413	0.8436
Rank	5.28	5.04	5.28	5.34	5.10	5.84	5.50	2.48	2.18	2.08

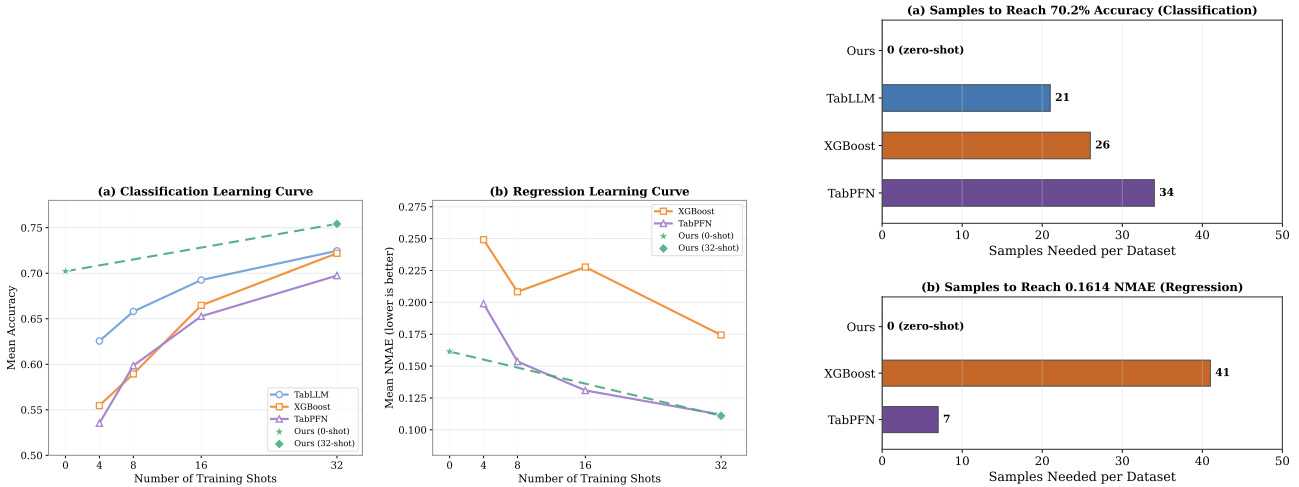
Reinforcing Numerical Reasoning in LLMs for Tabular Prediction via Structural Priors

Table 12. Accuracy (\uparrow) comparison across different models on classification datasets under zero-shot and few-shot settings. Darker green cells indicate higher accuracy. **TabLLM**, **TabPFN** and **XGBoost** are trained and evaluated under **few-shot** settings, while **Ours** and other LLM-based methods perform in-context **zero-shot** and **32-shot** inference without any task-specific training.

Dataset	Qwen-2.5-7B	Qwen-2.5-32B	Qwen3-8B	Qwen3-32B	Qwen3-235B	DS-R1	DS-0528	TabLLM				XGBoost				TabPFN				Ours		
								4 shot	8 shot	16 shot	32 shot	4 shot	8 shot	16 shot	32 shot	4 shot	8 shot	16 shot	32 shot	zero shot	32 shot	
adult	0.6700	0.7350	0.7250	0.7600	0.7550	0.7900	0.7600	0.7600	0.7600	0.4500	0.4737	0.6100	0.6900	0.6950	0.7100	0.4780	0.5497	0.6355	0.7047	0.7800	0.7950	
airfl	0.4400	0.3400	0.5600	0.5250	0.5300	0.5450	0.5500	0.4450	0.4450	0.4516	0.4993	0.4500	0.5300	0.5400	0.4950	0.4795	0.5022	0.5035	0.5082	0.5500	0.5550	
anac	0.1458	0.1667	0.5833	0.5417	0.7917	0.8333	0.3542	0.8750	0.8750	0.4811	0.5000	0.8333	0.7500	0.4792	0.8750	0.5400	0.6274	0.6747	0.7874	0.6875	0.8750	
annea	0.2444	0.3778	0.4111	0.2778	0.5556	0.4333	0.2889	0.7667	0.7667	0.5000	0.5000	0.6889	0.4111	0.7778	0.8667	0.0000	0.0000	0.0000	0.0000	0.7556	0.7667	
airhm	0.6739	0.5870	0.5435	0.5435	0.5652	0.6087	0.6304	0.4348	0.5870	0.5000	0.5161	0.5652	0.4348	0.5435	0.5000	0.5220	0.5264	0.6231	0.6220	0.5652	0.6304	
autoM	0.5500	0.7000	0.7250	0.7000	0.8500	0.8000	0.7000	0.5250	0.5250	0.5000	0.5284	0.5500	0.7500	0.7500	0.8250	0.7600	0.8337	0.8638	0.8650	0.7750	0.8250	
Bank	0.7290	0.7480	0.4530	0.4050	0.4430	0.4110	0.3870	0.7960	0.7960	0.5000	0.5450	0.2450	0.4410	0.5500	0.6930	0.4263	0.5611	0.5682	0.6456	0.7960	0.7960	
blast	0.7149	0.7674	0.6000	0.6213	0.6099	0.6227	0.5489	0.4000	0.7348	0.5000	0.5500	0.4780	0.4227	0.6610	0.7007	0.5386	0.5505	0.6337	0.6971	0.7348	0.7348	
brazi	0.6429	0.6190	0.3810	0.3571	0.3333	0.5238	0.2857	0.7619	0.7619	0.5007	0.5500	0.7381	0.7143	0.5000	0.5000	0.5361	0.5880	0.5747	0.6723	0.7619	0.7619	
calif	0.6200	0.3650	0.6700	0.7200	0.7700	0.5050	0.5000	0.5000	0.5000	0.5100	0.5550	0.5100	0.5950	0.7350	0.7450	0.5493	0.6597	0.7027	0.7718	0.7000	0.7450	
churn	0.4839	0.4516	0.4516	0.4516	0.4516	0.5161	0.4516	0.4516	0.4516	0.5263	0.5870	0.5484	0.3548	0.4194	0.4516	0.5262	0.5115	0.5344	0.5410	0.5161	0.6161	
chole	0.7840	0.7920	0.7480	0.5680	0.6900	0.5040	0.7340	0.1420	0.5800	0.5435	0.6494	0.7560	0.6460	0.1800	0.6820	0.4147	0.4433	0.5414	0.5901	0.8580	0.8580	
cleve	0.6774	0.7097	0.4839	0.5484	0.5806	0.4839	0.5806	0.4516	0.7742	0.5445	0.6400	0.6452	0.5806	0.8065	0.7097	0.5852	0.6361	0.7197	0.7672	0.6774	0.8419	
colic	0.3784	0.5405	0.6216	0.6216	0.6486	0.7568	0.5946	0.6216	0.6216	0.5484	0.6429	0.4054	0.6486	0.7297	0.7297	0.5284	0.7108	0.7932	0.8216	0.5946	0.8297	
commu	0.5950	0.6300	0.6800	0.7000	0.6550	0.6100	0.6000	0.5750	0.4250	0.5850	0.6429	0.5950	0.7300	0.7600	0.7900	0.5935	0.7020	0.7644	0.7875	0.6400	0.8300	
compa	0.3920	0.4792	0.5814	0.6212	0.5947	0.5852	0.6023	0.4697	0.4830	0.6000	0.6456	0.5417	0.5303	0.4811	0.5701	0.5203	0.5413	0.5312	0.5937	0.6420	0.6307	
dgb	0.6082	0.4561	0.8216	0.7778	0.8129	0.8450	0.7398	0.8363	0.8363	0.6216	0.6493	0.1813	0.7368	0.8947	0.8743	0.4220	0.7726	0.8158	0.8873	0.8363	0.8363	
diagf	0.6234	0.6623	0.6753	0.5974	0.6234	0.6234	0.6104	0.3506	0.4675	0.6216	0.6494	0.7662	0.6494	0.6753	0.6883	0.5630	0.6604	0.6162	0.6474	0.7662	0.7494	
diffie	0.7436	0.7949	0.8974	0.8462	0.9487	0.9487	0.7436	0.7692	0.7179	0.6250	0.6500	0.8974	0.8974	0.8974	0.9231	0.8195	0.8688	0.8818	0.9195	0.8974	0.9231	
Emplo	0.5408	0.6609	0.5429	0.5880	0.5300	0.3562	0.4517	0.3433	0.3433	0.6429	0.6550	0.6416	0.5794	0.6545	0.5814	0.6404	0.6161	0.6291	0.6502	0.6567	0.6567	
eye	0.5007	0.5007	0.4993	0.4665	0.4599	0.4796	0.5033	0.5007	0.5007	0.6456	0.6567	0.5138	0.5085	0.4915	0.5020	0.5007	0.5003	0.5168	0.5138	0.5059	0.4993	
flags	0.7000	0.5500	0.6000	0.5000	0.4500	0.4000	0.4500	0.5000	0.6500	0.6490	0.6875	0.3000	0.3000	0.4000	0.4000	0.4282	0.5128	0.5846	0.6205	0.6000	0.6500	
hayes	0.6429	0.5000	0.6429	0.6429	0.6429	0.4286	0.7857	0.6429	0.6429	0.6493	0.7143	0.3571	0.7143	0.7857	0.8571	0.5222	0.5556	0.5963	0.6667	0.6429	0.6729	
hepat	0.2500	0.5000	0.4375	0.3125	0.5000	0.5000	0.3750	0.8125	0.8125	0.6500	0.7404	0.5625	0.6250	0.5625	0.6250	0.5781	0.7387	0.7323	0.7484	0.8750	0.8750	
HMEQ	0.6376	0.7886	0.4262	0.5101	0.5268	0.3792	0.7097	0.8003	0.8003	0.6550	0.7412	0.7987	0.5923	0.5000	0.7450	0.4859	0.5800	0.6525	0.7255	0.8020	0.7987	
hypot	0.4683	0.7063	0.4127	0.5344	0.4524	0.3704	0.3651	0.9233	0.9233	0.6567	0.7433	0.7593	0.5344	0.8466	0.8148	0.0000	0.0000	0.0000	0.0000	0.6561	0.9153	
ibm	0.7755	0.7823	0.3401	0.3741	0.3878	0.2585	0.3469	0.8367	0.8367	0.6857	0.7500	0.6122	0.2585	0.6054	0.7551	0.5143	0.4810	0.5469	0.5344	0.8367	0.8367	
jungl	0.4407	0.7415	0.6992	0.7161	0.7288	0.7076	0.6780	0.4407	0.4407	0.7348	0.7667	0.4430	0.5932	0.6483	0.7585	0.8263	0.6257	0.6711	0.7985	0.9361	0.6398	0.7373
kc2	0.4340	0.3774	0.2453	0.2642	0.5094	0.4528	0.3208	0.7925	0.7925	0.7348	0.7619	0.2830	0.5283	0.6226	0.7170	0.6210	0.6714	0.6381	0.7562	0.7925	0.7925	
kdd	0.6456	0.6203	0.5443	0.6076	0.6203	0.5190	0.6076	0.4557	0.4557	0.7412	0.7667	0.4430	0.3671	0.8481	0.8608	0.5287	0.7102	0.7879	0.8293	0.5696	0.8456	
lungc	0.6522	0.7826	0.3043	0.2609	0.3043	0.1739	0.4783	0.8261	0.8261	0.7500	0.7800	0.4783	0.7826	0.5652	0.4783	0.4783	0.5696	0.6239	0.7196	0.8696	0.8696	
NATIC	0.6427	0.6293	0.6653	0.6467	0.6307	0.1893	0.6547	0.6493	0.6493	0.7570	0.7925	0.6787	0.8640	0.8120	0.8587	0.5857	0.6758	0.7800	0.8517	0.6480	0.8493	
newto	0.4286	0.5000	0.5714	0.5714	0.5000	0.4286	0.5714	0.5000	0.3571	0.7600	0.7947	0.4286	0.5000	0.7143	0.6429	0.4821	0.5571	0.6107	0.6679	0.6429	0.8133	
no2	0.5000	0.4600	0.5000	0.4800	0.4800	0.5000	0.5000	0.5000	0.5000	0.7600	0.7660	0.4800	0.4400	0.5200	0.6600	0.5100	0.5110	0.5280	0.5210	0.5200	0.8205	
page	0.5912	0.9033	0.6642	0.7810	0.8978	0.8631	0.4380	0.8978	0.8978	0.7619	0.8000	0.2464	0.8869	0.6387	0.8066	0.7836	0.8520	0.9093	0.9310	0.8704	0.8978	
phary	0.5500	0.5500	0.6000	0.4500	0.3500	0.4500	0.5000	0.6000	0.6000	0.7667	0.8003	0.7500	0.6000	0.6000	0.5000	0.6154	0.8657	0.7385	0.7513	0.6000	0.6000	
pm10	0.4800	0.5000	0.5000	0.5000	0.5000	0.4800	0.5000	0.5000	0.5000	0.7925	0.8108	0.5000	0.6200	0.5600	0.5000	0.4980	0.5020	0.5200	0.5140	0.5000	0.5000	
PostP	0.5298	0.6026	0.5894	0.5894	0.5629	0.6225	0.5894	0.6490	0.6490	0.7960	0.8156	0.7417	0.4702	0.7682	0.7748	0.5934	0.6095	0.6890	0.7684	0.6689	0.6490	
prn	0.1000	0.2000	0.5500	0.8000	0.4000	0.5000	0.3500	0.5000	0.5000	0.8003	0.8261	0.5500	0.5500	0.6500	0.8000	0.5175	0.8025	0.9800	1.0000	0.5500	0.5000	
road	0.5350	0.3300	0.3500	0.6400	0.5400	0.5550	0.4000	0.5100	0.5000	0.8125	0.8363	0.5000	0.6400	0.5300	0.6300	0.5390	0.5545	0.5577	0.5565	0.6500	0.6850	
segme	0.8225	0.7186	0.4848	0.8528	0.8442	0.8355	0.8442	0.8571	0.8571	0.8261	0.8367	0.3247	0.6364	0.9697	0.8918	0.5929	0.6781	0.7993	0.9591	0.7922	0.8571	
Skin	0.7043	0.8565	0.8652	0.8174	0.8652	0.8870	0.8565	0.9261	0.9261	0.8363	0.8387	0.9174	0.9261	0.9435	0.9261	0.6576	0.7172	0.7593	0.8787	0.9174	0.9043	
spamb	0.6052	0.7657	0.6161	0.5748	0.6920	0.5141	0.6703	0.6052	0.6052	0.8367	0.8563	0.6334	0.5597	0.8178	0.8330	0.5544	0.7403	0.8347	0.8510	0.7137	0.7202	
SPECT	0.7143	0.5143	0.7429	0.6571	0.7143	0.7143	0.6857	0.7143	0.7143	0.8563	0.8571	0.6286	0.6571	0.6571	0.6286	0.5800	0.6814	0.6986	0.7271	0.7143	0.7143	
spect	0.8889	0.7778	0.8889	0.1852	0.6481	0.1667	0.6111	0.8889	0.8889	0.8571	0.8580	0.1481	0.3519	0.9259	0.8704	0.5869	0.6963	0.8280	0.8738	0.7222	0.8889	
telic	0.6411	0.7518	0.5702	0.5957	0.6241	0.6071	0.5901	0.2780	0.7348	0.8580	0.8644	0.5021	0.4936	0.6950	0.6624	0.5313	0.5662	0.6241	0.6977	0.7362	0.7348	
Tour	0.6562	0.5833	0.3958	0.3438	0.3854	0.3125	0.3438	0.7604	0.7604	0.8750	0.8750	0.7292	0.4792	0.7396	0.7188	0.6236	0.6298	0.6812	0.6942	0.6604	0.7604	
triaz	0.5263	0.5263	0.4737	0.4737	0.4211	0.4211	0.5263	0.5809	0.3684	0.8889	0.8889	0.5263	0.6842	0.7368	0.7895	0.4895	0.5395	0.5605	0.6500	0.6316	0.5789	
Tumin	0.3750	0.3750	0.3750	0.3125	0.3750	0.0625	0.3750	0.6250	0.6250	0.8974	0.8957	0.6875	0.6250	0.625								

Table 14. NMAE (\downarrow) comparison across different models on regression datasets under zero-shot and few-shot settings. Darker green cells indicate lower NMAE. **TabPFN** and **XGBoost** are trained and evaluated under **few-shot** settings, while **Ours** and other LLM-based methods perform in-context **zero-shot** and **32-shot** inference without any task-specific training.

Dataset	Qwen-2.5-7B	Qwen-2.5-32B	Qwen3-8B	Qwen3-32B	Qwen3-235B	DS-R1	DS-0528	XGBoost				TabPFN				Ours	
								4 shot	8 shot	16 shot	32 shot	4 shot	8 shot	16 shot	32 shot	zero shot	32 shot
ames	0.0839	0.0997	0.0919	0.0578	0.0635	0.0605	0.1009	0.2751	0.0926	0.0777	0.0858	0.1003	0.0706	0.0541	0.0432	0.0868	0.0335
aucti	0.1831	0.1838	0.1804	0.1816	0.1819	0.1826	0.1846	0.3189	0.2286	0.1876	0.3318	0.1931	0.1879	0.1512	0.0732	0.1829	0.0828
Bosto	0.1346	0.1121	0.1506	0.1360	0.0619	0.0675	43.1375	0.2525	0.1170	0.1077	0.0794	0.1856	0.1127	0.0782	0.0756	0.1251	0.0687
cars	0.3299	0.2764	0.3575	0.2941	0.3314	0.2907	0.4177	0.0974	0.0905	0.0867	0.0469	0.1790	0.1578	0.1051	0.0681	0.1567	0.0584
colre	0.2892	0.2378	0.3233	1.0247	1.1183	0.4831	0.8425	0.2406	0.1890	0.1710	0.2072	0.3113	0.2052	0.1733	0.1420	0.2426	0.0906
concr	0.2237	0.1704	0.1961	0.2316	0.1106	0.1139	0.1685	0.2326	0.1630	0.1661	0.1230	0.1829	0.1567	0.1194	0.0851	0.1685	0.1499
CPMP	0.3852	0.3860	0.3854	0.3835	0.3845	0.3793	0.3856	0.4157	0.6947	0.5518	0.4200	0.3977	0.3880	0.3705	0.3780	0.3855	0.2864
emplo	0.1665	0.1804	0.0599	0.1034	0.0697	0.0418	0.1888	0.1216	0.1249	0.0746	0.0642	0.1048	0.0720	0.0506	0.0285	0.0860	0.0209
health	0.1836	0.1512	0.1537	0.1247	0.1517	0.1478	0.1656	0.4697	0.2409	0.1843	0.1023	0.2098	0.1501	0.1005	0.0828	0.1503	0.0947
house	0.0937	0.0675	0.0571	0.0578	0.0405	0.0774	0.0697	0.2050	0.0715	0.0660	0.0574	0.0890	0.0691	0.0510	0.0381	0.0632	0.0651
Lisbo	0.1661	0.3716	0.3182	0.1666	0.1269	0.1269	0.6827	0.1881	0.2410	0.2204	0.1948	0.1744	0.1298	0.1125	0.0918	0.1267	0.0570
lowbw	0.1755	0.1520	0.2667	0.1732	0.1393	0.1268	0.2929	0.1541	0.1797	0.1601	0.1683	0.2024	0.1490	0.1275	0.1171	0.1759	0.1592
mauna	0.2041	0.0333	0.0573	0.0352	0.0244	0.0246	0.0832	0.1577	0.1278	0.0779	0.0696	0.1126	0.0445	0.0298	0.0303	0.0508	0.0531
newto	0.4029	1.6552	0.8940	0.3716	0.3384	0.3670	0.5957	0.2934	0.2184	0.2649	0.3309	0.2807	0.2521	0.2307	0.2001	0.2429	0.2857
NHANE	0.2972	0.2798	0.2676	0.2925	0.2644	0.2652	0.2933	0.4441	0.3740	0.3218	0.3794	0.2833	0.2602	0.2502	0.2299	0.2636	0.1861
place	0.1765	0.5358	0.5702	0.4590	0.4478	0.4549	0.3526	0.1953	0.2105	0.4233	0.1866	0.2181	0.1899	0.1740	0.1653	0.1925	0.1618
pm10	0.1888	0.1992	0.1909	0.1893	0.1819	0.1883	0.2176	0.2090	0.1736	0.1809	0.2337	0.2220	0.1681	0.1591	0.1457	0.1891	0.1202
seoul	0.1747	0.1223	0.1412	0.1181	0.1088	0.1110	0.1333	0.1644	0.2444	0.5734	0.1514	0.1531	0.1690	0.1306	0.1095	0.1326	0.1219
std	0.2026	1.2481	0.2262	0.3650	0.9962	1.2384	0.7261	0.2380	0.2125	0.5603	0.2984	0.2429	0.2114	0.2146	0.2045	0.2238	0.2005
weath	0.0325	0.0325	0.0325	0.0642	0.0324	0.0325	0.0325	0.1638	0.1558	0.0610	0.0612	0.1360	0.0371	0.0264	0.0207	0.0325	0.0125
yacht	0.1502	0.1112	0.1396	0.1475	0.1673	0.1106	0.1425	0.3972	0.2245	0.2645	0.0695	0.1998	0.0434	0.0400	0.0207	0.1113	0.0216
Mean	0.2021	0.3146	0.2409	0.2370	0.2544	0.2329	2.3435	0.2492	0.2083	0.2277	0.1744	0.1990	0.1536	0.1309	0.1119	0.1614	0.1110
Rank i	11.05	10.76	10.81	9.86	7.24	7.24	13.10	13.14	11.33	10.33	9.19	12.52	7.43	3.71	2.00	8.19	3.10



(a) Few-shot learning curves on (a) classification and (b) regression tasks. While baseline models (TabLlM, XGBoost, TabPFN) require increasing amounts of labeled data to improve performance, our method achieves strong results in the zero-shot setting (star marker), surpassing the 16-shot performance of all baselines on classification tasks.

(b) Data efficiency under the zero-shot/few-shot setting: labeled samples required for baselines to match our zero-shot performance on (a) 53 classification and (b) 21 regression datasets. Sample counts are estimated via linear interpolation from 4/8/16/32-shot results.